Table 2. Dengue viraemia levels in plasma samples from marmosets after secondary and primary inoculation with DENV-1

Experiment/animal ID	Viraemia (log_{10} p.f.u. ml^{-1}) as determined in BHK/FcγR-expressing BHK cells at indicated day p.i.*				
	0	2	4	7	10
Secondary heterotypic inoculation (primary DENV-2, secondary DENV-1)					
Experiment 2					
D2D1-2	−/−	−/−	−/2.4	−/−	−/−
D2D1-3	−/−	−/−	−/−	−/2.4	−/−
D2D1-4	−/−	−/−	−/2.4	−/ 2.9	−/−
Experiment 3					
D2D1-5	−/−	2.8/3.8	2.8/4.3	−/−	−/−
D2D1-6	−/−	3.3/4.0	3.0/4.4	−/−	−/−
Primary inoculation (primary DENV-1)					
Experiment 5					
D1-1	−/−	4.8/4.4	4.1/3.8	3.8/−	−/−
D1-2	−/−	4.4/4.7	4.7/4.4	4.4/2.7	−/−

*A '−' indicates viraemia below detection levels (<2.0 log_{10} p.f.u. ml^{-1}).

levels of viraemia were found with both BHK and FcγR-expressing BHK cells (Table 2, experiment 5). These findings are consistent with results obtained using serum samples from human patients with secondary DENV infection (Moi *et al.*, 2011). The results suggested that infectious DENV–antibody complexes are present during secondary DENV infection, and that these complexes can be detected with FcγR-expressing BHK cells but not with BHK cells (which are FcγR negative).

IgM and IgG antibody responses in marmosets after secondary DENV inoculation

Antibody responses after secondary DENV infection were analysed and compared with those after primary infection (Table 3). IgM was first detected at day 4 after primary inoculation. As reported previously (Omatsu *et al.*, 2011), IgM levels increased rapidly from day 7 (Table 3, experiment 5; Fig. 1). In the case of secondary infection, IgM was first detected at day 7 or 10 after secondary inoculation (Table 3, experiments 1–4). The IgM levels increased but were lower than those in primary infection (Fig. 1b). The mean positive : negative (P : N) ratio for IgM was higher for marmosets with primary infection (P : N=29.6) at 14 days p.i. than for those with secondary infection (P : N=10.4; Student's *t*-test, $P<0.01$).

IgG antibody responses were also analysed by ELISA (Table 4). IgG was first detected at day 7 or 14 after primary inoculation. The levels increased gradually (experiment 5). All marmosets that were inoculated previously with DENV were positive for IgG prior to the secondary inoculation. The IgG antibody levels increased rapidly from day 7 after primary inoculation (experiment 2). The mean IgG antibody level in marmosets with secondary infection (P : N=22.7) at 14 days p.i. was higher than that in marmosets with primary infection (P : N=10.3; Student's *t*-test, $P=0.04$). These results indicated that marmosets inoculated with heterotypic DENV exhibited secondary

Table 3. IgM antibody responses in marmosets following secondary infection with DENV

Results are shown as the P : N ratio. Positive detection of DENV IgM (P : N ⩾2.0) is indicated in bold.

Experiment/animal ID	Days p.i.						
	0	2	3	4	7	10	14
Secondary heterotypic inoculation							
Experiment 1 (primary DENV-3, secondary DENV-2)							
D3D2-1	0.7	NT	1.2	NT	**5.5**	NT	**15.3**
D3D2-2	1.5	NT	1.5	NT	**2.7**	NT	**15.0**
D3D2-3	0.9	NT	1.0	NT	1.7	NT	**6.1**
Experiment 2 (primary DENV-2, secondary DENV-1)							
D2D1-1	0.8	1.1	NT	1.3	1.6	**2.0**	**7.9**
D2D1-2	0.9	0.8	NT	0.8	1.1	**3.5**	**6.2**
D2D1-3	0.6	0.6	NT	0.7	0.6	**2.3**	**11.7**
D2D1-4	0.9	0.6	NT	0.9	1.2	**4.3**	**12.7**
Experiment 3 (primary DENV-2, secondary DENV-1)							
D2D1-5	1.3	1.1	NT	1.1	**2.0**	**4.8**	**8.5**
D2D1-6	1.3	1.2	NT	1.4	**3.2**	**8.4**	**15.0**
Experiment 4 (primary DENV-2, secondary DENV-3)							
D2D3-1	1.5	1.5	NT	1.4	1.9	**2.1**	**9.6**
D2D3-2	1.0	0.9	NT	1.0	**2.7**	**2.5**	**6.6**
Primary inoculation							
Experiment 5 (primary DENV-1)							
D1-1	1.2	1.3	NT	**2.0**	**17.5**	**27.5**	**29.4**
D1-2	0.5	0.5	NT	1.0	**15.3**	**29.4**	**29.8**

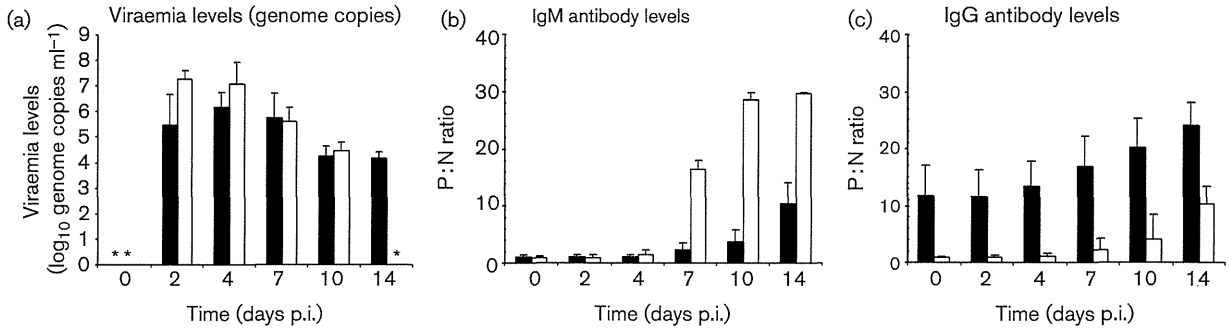

Fig. 1. Viraemia kinetics and antibody response in DENV-inoculated marmosets. (a) Viraemia levels as determined by reverse transcriptase-PCR. (b,c) IgM (b) and IgG (c) antibody levels during primary and secondary infection in marmosets. Filled bars indicate secondary heterologous infection (experiments 1–4) and open bars indicate primary infection (experiment 5). P:N ratio, positive : negative ratio. Asterisks indicate values below the detection level.

IgM and IgG responses that were consistent with those found in human DENV infection (Fig. 1).

Neutralizing antibody responses in marmosets after secondary DENV inoculation

Levels of neutralizing antibody to all four DENV serotypes were examined at days 0, 4, 7, 10 and 14 p.i. in primary (D1-1 and D1-2) and heterologous secondary (D2D1-1, D2D1-2, D2D1-3, D2D1-4, D2D1-5, D2D1-6, D2D3-1 and D2D3-2) infections using BHK cells and FcγR-expressing BHK cells (Table 5). Neutralizing antibody to DENV-2 was detected at day 0 in four of eight marmosets that received DENV-2 in the primary inoculation (experiments 2–4). Following secondary inoculation with DENV-1 or DENV-3, serotype cross-reactive antibodies were first detected as early as day 4. The levels increased rapidly in four marmosets (D2D1-5, D2D1-6, D2D3-1 and D2D3-2), which had undetectable levels of DENV neutralizing antibodies on the day of secondary inoculation (day 0). At day 14 after secondary inoculation, neutralizing antibody to four serotypes was detected in all marmosets with secondary infection by an assay using BHK and FcγR-expressing BHK cells (Table 5, experiments 2–4). After heterotypic secondary infection, however, neutralizing antibody titres were found to be higher when assayed using BHK cells than when using FcγR-expressing BHK cells. Following primary inoculation with DENV-1, neutralizing antibody titre was first detected at day 7, and was highest to DENV-1 (experiment 5). The results suggested that neutralizing antibody responses of marmosets after both primary inoculation and secondary inoculation with heterologous serotypes were consistent with neutralizing antibody responses in humans. As seen in human DENV infection, serotype cross-reactive antibodies were detected during the early phase of secondary infection when using FcγR-negative cells, but the titres were lower or undetectable when using FcγR-expressing cells. The discrepancies between the two types of assay in neutralizing antibody titres were also consistent with the discrepancies of the same two assays when they are applied to humans.

Table 4. IgG responses in marmosets following secondary infection with DENV

Results are shown as the P:N ratio. Positive detection of DENV IgG (P:N ≥2.0) is indicated in bold.

Experiment/ animal ID	Days p.i.						
	0	2	3	4	7	10	14
Secondary heterotypic inoculation							
Experiment 1 (primary DENV-3, secondary DENV-2)							
D3D2-1	**5.0**	NT	**5.7**	NT	**14.5**	NT	**21.7**
D3D2-2	**6.9**	NT	**6.6**	NT	**12.5**	NT	**17.2**
D3D2-3	**4.6**	NT	**4.5**	NT	**4.7**	NT	**14.2**
Experiment 2 (primary DENV-2, secondary DENV-1)							
D2D1-1	**19.5**	**17.8**	NT	**20.2**	**19.5**	**21.6**	**26.3**
D2D1-2	**18.9**	**18.3**	NT	**19.0**	**23.4**	**28.9**	**28.9**
D2D1-3	**13.1**	**13.8**	NT	**13.9**	**16.8**	**23.9**	**28.1**
D2D1-4	**17.3**	**15.1**	NT	**16.1**	**23.8**	**28.2**	**27.8**
Experiment 3 (primary DENV-2, secondary DENV-1)							
D2D1-5	**12.0**	**12.2**	NT	**12.0**	**8.4**	**17.1**	**19.0**
D2D1-6	**6.6**	**7.1**	NT	**8.0**	**17.4**	**19.3**	**19.5**
Experiment 4 (primary DENV-2, secondary DENV-3)							
D2D3-1	**11.2**	**11.6**	NT	**11.9**	**11.9**	**14.6**	**21.0**
D2D3-2	**13.2**	**13.7**	NT	**14.1**	**13.7**	**15.4**	**21.3**
Primary inoculation							
Experiment 5 (primary DENV-1)							
D1-1	0.6	0.7	NT	0.7	0.7	1.0	**8.1**
D1-2	1.1	1.2	NT	1.4	**3.6**	**7.2**	**12.4**

DISCUSSION

Although we have reported previously on the utility of the marmoset model in the analysis of primary DENV infection (Moi *et al.*, 2013; Omatsu *et al.*, 2011, 2012), its

Table 5. Neutralizing antibody titres to the four DENV serotypes after secondary DENV infection, determined by using BHK and FcγR-expressing BHK cells

Results are shown as 50 % plaque reduction neutralization test ($PRNT_{50}$) values, expressed as the reciprocal of the highest plasma dilution (end-point titre) that results in ⩽50% of input plaque count (WHO, 2009); NT, not performed. PRNT was not performed for marmosets in experiment 1 due to a low sample volume.

Animal ID	Serotype used for inoculation		PRNT challenge virus	BHK cells at indicated days p.i.					FcγR-expressing BHK cells at indicated days p.i.				
	First inoculation	Second inoculation		0	4	7	10	14	0	4	7	10	14
Experiment 2													
D2D1-1	DENV-2	DENV-1	DENV-1	<20	NT	<20	<20	40	<20	<20	<20	<20	40
			DENV-2	160	160	160	160	320	80	80	80	160	80
			DENV-3	40	40	20	80	160	<20	NT	<20	<20	<20
			DENV-4	<20	80	20	80	80	<20	<20	<20	40	40
D2D1-2	DENV-2	DENV-1	DENV-1	20	NT	20	160	80	<20	<20	<20	<20	80
			DENV-2	20	40	80	160	160	20	20	40	40	20
			DENV-3	40	40	NT	NT	160	<20	<20	<20	<20	20
			DENV-4	<20	<20	<20	160	80	<20	<20	<20	80	80
D2D1-3	DENV-2	DENV-1	DENV-1	<20	<20	<20	20	20	<20	<20	<20	<20	40
			DENV-2	40	40	40	320	160	80	20	80	20	80
			DENV-3	40	20	NT	20	160	<20	<20	<20	<20	160
			DENV-4	<20	<20	<20	40	160	<20	<20	<20	40	160
D2D1-4	DENV-2	DENV-1	DENV-1	<20	<20	<20	<20	160	<20	<20	<20	<20	40
			DENV-2	20	80	20	20	160	<20	40	NT	40	80
			DENV-3	40	20	80	80	160	<20	NT	<20	<20	160
			DENV-4	<20	<20	<20	160	160	<20	<20	<20	40	80
Experiment 3													
D2D1-5	DENV-2	DENV-1	DENV-1	<20	<20	20	160	320	<20	<20	<20	20	80
			DENV-2	<20	20	80	20	40	<20	20	80	160	40
			DENV-3	<20	20	160	160	320	<20	20	160	40	160
			DENV-4	20	NT	80	20	80	<20	<20	<20	<20	80
D2D1-6	DENV-2	DENV-1	DENV-1	<20	<20	NT	20	160	<20	<20	<20	<20	80
			DENV-2	<20	20	40	NT	20	<20	20	20	80	20
			DENV-3	<20	40	80	160	160	<20	<20	NT	20	40
			DENV-4	<20	80	160	40	80	<20	<20	80	20	40
Experiment 4													
D2D3-1	DENV-2	DENV-3	DENV-1	<20	<20	80	NT	80	<20	<20	<20	<20	80
			DENV-2	<20	40	80	80	40	<20	40	80	40	40
			DENV-3	<20	40	80	80	320	<20	20	40	40	80
			DENV-4	<20	NT	80	NT	80	<20	NT	NT	NT	40
D2D3-2	DENV-2	DENV-3	DENV-1	<20	40	160	NT	160	<20	<20	<20	<20	80
			DENV-2	<20	40	80	20	40	<20	40	80	80	20
			DENV-3	<20	NT	80	NT	160	<20	<20	80	NT	80
			DENV-4	<20	80	80	NT	40	<20	NT	80	NT	40

Table 5. cont.

Animal ID	Serotype used for inoculation		PRNT challenge virus	BHK cells at indicated days p.i.				FcγR-expressing BHK cells at indicated days p.i.				
	First inoculation	Second inoculation		0	4	7	10	14	0	4	7	10	14
Experiment 5													
D1-1	DENV-1	–	DENV-1	<20	<20	NT	80	160	<20	<20	80	80	80
			DENV-2	<20	<20	<20	<20	40	<20	<20	<20	<20	40
			DENV-3	<20	<20	<20	80	40	<20	<20	<20	<20	<20
			DENV-4	<20	<20	20	20	80	<20	<20	NT	<20	40
D1-2	DENV-1	–	DENV-1	<20	<20	<20	40	320	<20	<20	<20	20	80
			DENV-2	<20	<20	<20	<20	20	<20	<20	<20	<20	<20
			DENV-3	<20	<20	40	80	160	<20	<20	<20	80	40
			DENV-4	<20	<20	20	40	80	<20	NT	<20	20	<20

utility as a model for secondary DENV infection had not been confirmed. In the present study, viraemia and antibody responses in marmosets were analysed after secondary infection with heterotypic serotypes of DENV. The response exhibited in marmosets was similar to that in humans in that infection with one serotype did not confer protection to others. This was shown by the viraemia present in previously infected marmosets when they were infected with a different DENV serotype. High levels of viraemia were consistently detected in all of the marmosets after secondary DENV-1 and DENV-3 infection (Table 1), and virus titres were as high as 7 $\log_{10}$ genome copies ml^{-1}. The mean peak levels of viraemia, as detected by reverse transcription-PCR, did not differ significantly between primary and secondary DENV infection. In three marmosets, viraemia was detected for a longer duration (up to day 14 after secondary inoculation; Table 1). In an earlier study, which used 20 marmosets, none of the animals exhibited viraemia beyond day 10 after primary DENV inoculation (Omatsu *et al.*, 2011). Peak viraemia titres in macaques with secondary DENV-1 infection were reported to range from undetectable to 4 log p.f.u. in 0.5 ml (Halstead *et al.*, 1973a). Additionally, viraemia was also variable in white-handed gibbons with heterologous secondary DENV infection; viraemia was undetectable in some animals with heterologous secondary DENV infection (Whitehead *et al.*, 1970). In comparison, viraemia was detected in all marmosets (Table 1), and peak viraemia titres in marmosets with secondary DENV-1 infection ranged from 2.4 to 4.4 $\log_{10}$ p.f.u. ml^{-1} (Table 2). The results demonstrated that marmosets consistently develop viraemia after secondary infection with heterologous DENV. The results also indicated that protective immunity to heterologous serotypes was absent. The results suggested that the peak viraemia titres in marmosets is not as high as those in human DENV infection (Moi *et al.*, 2011), and further studies using a larger number of marmosets and manipulation of the marmoset model are needed to address the clinical and pathophysiological aspects of heterologous secondary infection in marmosets. Overall, the results suggest that marmosets could provide a reliable model for therapeutics and vaccine evaluation studies.

The antibody responses in DENV-infected humans have been well studied (Anantapreecha *et al.*, 2005, 2007; reviewed by Rothman, 2010; WHO, 2009). Antibody responses differ between primary and secondary infections (WHO, 2009). In secondary infection, IgG and neutralizing antibody titres rise rapidly and are cross-reactive to all of the other DENV serotypes, whilst IgM levels are low or undetectable. In primary infection, IgM antibody is detected at the early phase (before IgG is detected), and the IgM levels are high. In the present study, IgG antibody was detected before secondary infection (day 0) in marmosets that had previously been infected with DENV. The IgG titres rose rapidly (as early as day 4 p.i.) to levels that were significantly higher than the titre levels in primary infection. These results, which suggest that IgG

antibodies and anamnestic memory persisted for more than a year (up to 83 weeks) after primary DENV inoculation, concur with the results of clinical studies in human dengue patients where DENV-specific IgG has been shown to remain detectable for up to a few years after primary infection (WHO, 2009). In experimentally infected marmosets, IgM levels were also significantly lower during secondary infection than they were in primary infection. Thus, IgM and IgG antibody responses in marmosets after secondary infection mimic the antibody responses seen in human DENV infection.

It is known that neutralizing antibodies induced after secondary DENV infection are cross-reactive to the four DENV serotypes in human dengue infections (de Alwis *et al.*, 2011; Xu *et al.*, 2012; Zompi *et al.*, 2012; reviewed by Guzman *et al.*, 2013; Zompi & Harris, 2013). After secondary DENV infection, the marmosets of the present study exhibited high levels of neutralizing antibody titres to challenge infection not only from the serotypes with which they had previously been infected but also from serotypes to which they had not. Primary infection with one DENV serotype induced serotype-specific antibodies, and elicited life-long immunity, but only to that serotype. Immunity to other serotypes was short-lived. As in humans, marmosets that had low neutralizing titres before secondary infection (day 0) were susceptible to infection with heterologous serotypes. High titres of serotype cross-reactive neutralizing antibodies were induced in marmosets after secondary infection with heterotypic serotypes. The results indicate consistency between humans and marmosets in the neutralizing antibody patterns present after secondary DENV infection.

When FcγR-expressing BHK cells were used, the viraemia titres that were detected in marmoset serum samples taken on days 2–7 after secondary infection were higher than those detected using BHK cells (Table 2). In samples from marmosets after primary DENV infection, the viraemia titres of assays using FcγR-expressing BHK cells and BHK cells did not differ. The fact that the detected levels of viraemia in serum samples from secondary infection were 10 times higher in assays using FcγR-expressing cells than they were in BHK cells suggests that infectious virus–antibody immune complexes are formed during secondary infection. The presence of infectious immune complexes during secondary infection in marmosets is also consistent with secondary DENV infections in humans (Moi *et al.*, 2011).

Animal challenge models afford methods to evaluate the efficacy of dengue vaccines and therapeutics. In the present study, the marmosets consistently developed viraemia and immune responses that mimicked those of secondary DENV infection in humans. Serotype cross-reactive antibody responses in marmosets during secondary DENV infection suggested the induction of strong T- and B-cell memories by primary DENV infection. Thus, our results suggest that marmosets are useful for vaccine efficacy studies, immune response studies and studies to better understand the immune mechanisms of protection and pathogenesis in secondary DENV infections.

METHODS

Ethics statement. All animal studies were conducted in accordance with the 'Guides for Animal Experiments Performed at National Institute of Infectious Diseases', approved by the Animal Welfare and Animal Care Committee of the National Institute of Infectious Diseases, Japan (approval nos 608011 and 609014), and the 'National Institute of Biomedical Innovation Rules and Guidelines for Experimental Animal Welfare', approved by the National Institute of Biomedical Innovation, Japan (approval nos 20-003 and 21-013). All animals were euthanized by cardiac exsanguination under pentobarbital-induced anaesthesia.

Animals. A total of 13 male marmosets were used. Marmosets were purchased from Clea Japan and caged singly at 27 ± 2 °C in 50 ± 10 % humidity with a 12 h light/dark cycle (lighting from 7:00 to 19:00) at the Tsukuba Primate Research Center, National Institute of Biomedical Innovation, Tsukuba, Japan. Animals were fed twice a day with a standard marmoset diet (Clea New World Monkey Diet, CMS-1M; Clea Japan) supplemented with fruit, eggs and milk. Water was provided *ad libitum*. The animals were in a healthy condition and were confirmed to be negative for anti-DENV antibodies before inoculation with DENV.

DENV strains and propagation. DENV-1 02-17, DENV-1 01-44, DENV-2 DHF0663 (GenBank accession no. AB189122) and DENV-3 DSS1403 were the strains used for inoculation studies (Moi *et al.*, 2012; Omatsu *et al.*, 2011). All DENV strains were used within four passages on C6/36 cells. The culture supernatant from infected C6/36 cells was centrifuged at 800*g* for 5 min to remove cell debris and stored at −80 °C until use.

Infection of marmosets. In experiment 1, three marmosets (D3D2-1, D3D2-2 and D3D2-3) were inoculated subcutaneously with 6 $\log_{10}$ p.f.u. DENV-3 DSS1403 for primary infection. Secondary inoculation with 7 log10 p.f.u. DENV-2 DHF0663 was administered 59 weeks (13 months) after the primary inoculation. In experiment 2, four marmosets were inoculated subcutaneously with 5 $\log_{10}$ p.f.u. DENV-2 for primary infection. Secondary inoculation with 6 $\log_{10}$ p.f.u. DENV-1 was administered 59 weeks (13 months) after the primary inoculation. Three of the four marmosets in experiment 2 (D2D1-1, D2D1-2 and D2D1-3) were inoculated with DENV-1 02-17, and one (D2D1-4) was inoculated with DENV-1 01-44. In experiment 3, two marmosets (D2D1-5 and D2D1-6) were inoculated subcutaneously with 4 $\log_{10}$ p.f.u. DENV-2 for primary infection. Secondary inoculation with 6 $\log_{10}$ p.f.u. DENV-1 was administered 83 weeks (19 months) after the first inoculation. In experiment 4, two marmosets (D2D3-1 and D2D3-2) were inoculated subcutaneously with 3 $\log_{10}$ p.f.u. DENV-2 for primary infection. Secondary inoculation with 6 $\log_{10}$ p.f.u. DENV-3 was administered 83 weeks (19 months) after the first inoculation. In experiment 5, which only examined primary infection, two marmosets (D1-1 and D1-2) were inoculated with DENV-1 (marmoset D1-1: DENV-1 02-17; marmoset D1-2: DENV-1 01-44). The amount of DENV transmitted by *Aedes aegypti* is reported to range from 3×10^2 to 2×10^5 50% mosquito infectious doses (Gubler & Rosen, 1976). Recent studies showed that levels as high as $>10^6$ p.f.u. DENV can be transmitted by mosquitoes (Styer *et al.*, 2007). In the present study, marmosets were inoculated with 10^6–10^7 p.f.u. DENV, which may be higher in comparison with levels transmitted by mosquitoes. All of the marmosets in the five experimental groups were observed for clinical signs at the time of blood collection. Blood samples were centrifuged at

200*g* for 10 min for plasma collection. Inoculation with DENV and blood drawing were performed under anaesthesia with 5 mg ketamine hydrochloride kg^{-1}. Day 0 was defined as the day of primary virus inoculation. Each marmoset was evaluated using similar virus and antibody titration methods and sampling intervals.

Quantification of viraemia by RT-PCR and plaque assay. Levels of dengue viral RNA in plasma and organ samples (High Pure Viral RNA kit, Roche Diagnostics) were determined by TaqMan real-time RT-PCR (Moi *et al.*, 2011). Viral titres determined by RT-PCR were expressed as genome copies ml^{-1}. Thirteen marmosets in experiments 1–5 were quantified for viral RNA using RT-PCR (Table 1). Of the 13 marmosets, plasma samples from seven marmosets were used for infectious virus quantification (experiments 2, 3 and 5) using BHK and FcγR-expressing BHK cells (Table 2). Due to the lack of plasma samples from marmosets of experiments 1 and 4 for infectious virus titration, quantification for viraemia using a cell-based assay could not be carried out for these experiments. To determine viraemia levels in plasma samples, the samples were serially diluted 10-fold from $1:10^1$ to $1:10^6$ with Eagle's minimum essential medium (Sigma) supplemented with 10 % FBS. Fifty microlitres of diluted plasma samples were inoculated onto BHK and FcγR-expressing BHK cell monolayers in 12-well plates. The plates were incubated for 1 h at 37 °C in 5 % CO_2. After virus adsorption, the cells were overlaid with maintenance medium containing 1 % methylcellulose (Wako Pure Chemical Industries). The plates were incubated at 37 °C in 5 % CO_2 until visible plaques could be observed (5–7 days of incubation). The cells were fixed, stained with methylene blue and washed with water. Assays were conducted in duplicate. Viral titres were expressed as p.f.u. ml^{-1} using the following formula: (number of plaques per well × dilution)/inoculum volume.

Serological studies. DENV-specific IgM antibody was detected using a Dengue Fever IgM Capture ELISA (Focus), and DENV-specific IgG antibody was examined using a Dengue IgG Indirect ELISA (PanBio) in accordance with the manufacturers' instructions. The P : N ratio was calculated by the formula: absorbance of the test sample/absorbance of a negative sample. Plasma samples collected from three DENV-naïve marmosets were used as the negative samples. P : N ratios of <2 and $\geqslant 2$ were considered to be negative and positive, respectively. All ELISAs were conducted in duplicate (Ito *et al.*, 2011).

Neutralizing antibody titres were determined by plaque reduction neutralization tests with four DENV strains (DENV-1 01-44, DENV-2 DHF0663, DENV-3 CH53489 and DENV-4 TVP360). Heat-inactivated plasma samples were serially diluted twofold from 1 : 10 to 1 : 640 with minimum essential medium (MEM) supplemented with 2 % FBS. Virus–antibody mixture was prepared by mixing 25 µl DENV at titres of 2000 p.f.u. ml^{-1} with 25 µl serially diluted serum samples to make up a final serum dilution of 1 : 20 to 1 : 1280. Control virus samples were prepared by mixing 25 µl DENV at titres of 2000 p.f.u. ml^{-1} with 25 µl MEM supplemented with 2 % FBS. Virus–antibody mixture was incubated at 37 °C for 1 h. Fifty microlitres of virus–antibody mixture was inoculated onto BHK and FcγR-expressing BHK cell monolayers in 12-well plates. After 5–7 days of inoculation the cells were fixed and stained, and the plaques were counted. A neutralizing assay was not carried out in some samples due to insufficient volume. Tests were conducted in duplicate. The neutralization titre was expressed as the maximum dilution of plasma sample that yielded a $\geqslant 50$ % plaque reduction in the virus inoculum in comparison with a control virus sample.

Statistics. Results were expressed as the mean value of each group. Student's *t*-test was used to compare the mean titres and determine statistical significance. The statistical package in Microsoft Excel was used for statistical calculations. A *P* value of <0.05 was considered to be statistically significant.

ACKNOWLEDGEMENTS

We thank Dr Jeffrey V. Ravetch, Rockefeller University, NY, USA for generously providing the FcγRIIA cDNA and Dr Susheela Tridandapani, Ohio State University College of Medicine, Columbus, OH, USA, for assistance in obtaining the FcγRIIA cDNA used in this work. This work was supported by grants from Research on Emerging and Re-emerging Infectious Diseases (H23-Shinkou-Ippan-010), from the Ministry of Health, Labour and Welfare, Japan, and a Grant-in-aid for Scientific Research from the Ministry of Education, Culture, Sports, Science and Technology of Japan (Kiban B no. 25293112 and 22390093, and Wakate B no. 23790515).

REFERENCES

Anantapreecha, S., Chanama, S., A-nuegoonpipat, A., Naemkhunthot, S., Sa-Ngasang, A., Sawanpanyalert, P. & Kurane, I. (2005). Serological and virological features of dengue fever and dengue haemorrhagic fever in Thailand from 1999 to 2002. *Epidemiol Infect* **133**, 503–507.

Anantapreecha, S., A-Nuegoonpipat, A., Prakrong, S., Chanama, S., Sa-Ngasang, A., Sawanpanyalert, P. & Kurane, I. (2007). Dengue virus cross-reactive hemagglutination inhibition antibody responses in patients with primary dengue virus infection. *Jpn J Infect Dis* **60**, 267–270.

Bente, D. A., Melkus, M. W., Garcia, J. V. & Rico-Hesse, R. (2005). Dengue fever in humanized NOD/SCID mice. *J Virol* **79**, 13797–13799.

Bernardo, L., Izquierdo, A., Prado, I., Rosario, D., Alvarez, M., Santana, E., Castro, J., Martínez, R., Rodríguez, R. & other authors (2008). Primary and secondary infections of *Macaca fascicularis* monkeys with Asian and American genotypes of dengue virus 2. *Clin Vaccine Immunol* **15**, 439–446.

Bhatt, S., Gething, P. W., Brady, O. J., Messina, J. P., Farlow, A. W., Moyes, C. L., Drake, J. M., Brownstein, J. S., Hoen, A. G. & other authors (2013). The global distribution and burden of dengue. *Nature* **496**, 504–507.

Clark, K. B., Onlamoon, N., Hsiao, H. M., Perng, G. C. & Villinger, F. (2013). Can non-human primates serve as models for investigating dengue disease pathogenesis? *Front Microbiol* **4**, 305.

de Alwis, R., Beltramello, M., Messer, W. B., Sukupolvi-Petty, S., Wahala, W. M. P. B., Kraus, A., Olivarez, N. P., Pham, Q., Brien, J. D. & other authors (2011). In-depth analysis of the antibody response of individuals exposed to primary dengue virus infection. *PLoS Negl Trop Dis* **5**, e1188.

Gubler, D. J. & Rosen, L. (1976). A simple technique for demonstrating transmission of dengue virus by mosquitoes without the use of vertebrate hosts. *Am J Trop Med Hyg* **25**, 146–150.

Guirakhoo, F., Pugachev, K., Arroyo, J., Miller, C., Zhang, Z. X., Weltzin, R., Georgakopoulos, K., Catalan, J., Ocran, S. & other authors (2002). Viremia and immunogenicity in nonhuman primates of a tetravalent yellow fever–dengue chimeric vaccine: genetic reconstructions, dose adjustment, and antibody responses against wild-type dengue virus isolates. *Virology* **298**, 146–159.

Guirakhoo, F., Pugachev, K., Zhang, Z., Myers, G., Levenbook, I., Draper, K., Lang, J., Ocran, S., Mitchell, F. & other authors (2004). Safety and efficacy of chimeric yellow fever–dengue virus tetravalent vaccine formulations in nonhuman primates. *J Virol* **78**, 4761–4775.

Guy, B., Barban, V., Mantel, N., Aguirre, M., Gulia, S., Pontvianne, J., Jourdier, T. M., Ramirez, L., Gregoire, V. & other authors (2009). Evaluation of interferences between dengue vaccine serotypes in a monkey model. *Am J Trop Med Hyg* **80**, 302–311.

Guzman, M. G., Alvarez, M. & Halstead, S. B. (2013). Secondary infection as a risk factor for dengue hemorrhagic fever/dengue shock syndrome: an historical perspective and role of antibody-dependent enhancement of infection. *Arch Virol* **158**, 1445–1459.

Halstead, S. B., Shotwell, H., Casals, J. & Clinical Laboratory Responses to Heterologous Infection (1973a). Studies on the pathogenesis of dengue infection in monkeys. II. Clinical laboratory responses to heterologous infection. *J Infect Dis* **128**, 15–22.

Halstead, S. B., Casals, J., Shotwell, H. & Palumbo, N. (1973b). Studies on the immunization of monkeys against dengue. I. Protection derived from single and sequential virus infections. *Am J Trop Med Hyg* **22**, 365–374.

Ito, M., Katakai, Y., Ono, F., Akari, H., Mukai, R. Z., Takasaki, T., Kotaki, A. & Kurane, I. (2011). Serotype-specific and cross-reactive neutralizing antibody responses in cynomolgus monkeys after infection with multiple dengue virus serotypes. *Arch Virol* **156**, 1073–1077.

Kochel, T. J., Watts, D. M., Gozalo, A. S., Ewing, D. F., Porter, K. R. & Russell, K. L. (2005). Cross-serotype neutralization of dengue virus in *Aotus nancymae* monkeys. *J Infect Dis* **191**, 1000–1004.

Koraka, P., Benton, S., van Amerongen, G., Stittelaar, K. J. & Osterhaus, A. D. (2007a). Efficacy of a live attenuated tetravalent candidate dengue vaccine in naïve and previously infected cynomolgus macaques. *Vaccine* **25**, 5409–5416.

Koraka, P., Benton, S., van Amerongen, G., Stittelaar, K. J. & Osterhaus, A. D. M. E. (2007b). Characterization of humoral and cellular immune responses in cynomolgus macaques upon primary and subsequent heterologous infections with dengue viruses. *Microbes Infect* **9**, 940–946.

Lubiniecki, A. S. & Tarr, G. C. (1977). Immunological sensitization following inapparent infection with dengue virus type 3 in rhesus monkeys. *Experientia* **33**, 330–331.

Marchette, N. J., Halstead, S. B., Falkler, W. A., Jr, Stenhouse, A. & Nash, D. (1973). Studies on the pathogenesis of dengue infection in monkeys. 3. Sequential distribution of virus in primary and heterologous infections. *J Infect Dis* **128**, 23–30.

Moi, M. L., Lim, C. K., Kotaki, A., Takasaki, T. & Kurane, I. (2011). Detection of higher levels of dengue viremia using FcγR-expressing BHK-21 cells than FcγR-negative cells in secondary infection but not in primary infection. *J Infect Dis* **203**, 1405–1414.

Moi, M. L., Lim, C. K., Chua, K. B., Takasaki, T. & Kurane, I. (2012). Dengue virus infection-enhancing activity in serum samples with neutralizing activity as determined by using FcγR-expressing cells. *PLoS Negl Trop Dis* **6**, e1536.

Moi, M. L., Omatsu, T., Hirayama, T., Nakamura, S., Katakai, Y., Yoshida, T., Saito, A., Tajima, S., Ito, M. & other authors (2013). Presence of viral genome in urine and development of hematuria and pathological changes in kidneys in common marmoset (*Callithrix jacchus*) after inoculation with dengue virus. *Pathogens* **2**, 357–363.

Omatsu, T., Moi, M. L., Hirayama, T., Takasaki, T., Nakamura, S., Tajima, S., Ito, M., Yoshida, T., Saito, A. & other authors (2011). Common marmoset (*Callithrix jacchus*) as a primate model of dengue virus infection: development of high levels of viraemia and demonstration of protective immunity. *J Gen Virol* **92**, 2272–2280.

Omatsu, T., Moi, M. L., Takasaki, T., Nakamura, S., Katakai, Y., Tajima, S., Ito, M., Yoshida, T., Saito, A. & other authors (2012). Changes in hematological and serum biochemical parameters in common marmosets (*Callithrix jacchus*) after inoculation with dengue virus. *J Med Primatol* **41**, 289–296.

Onlamoon, N., Noisakran, S., Hsiao, H. M., Duncan, A., Villinger, F., Ansari, A. A. & Perng, G. C. (2010). Dengue virus-induced hemorrhage in a nonhuman primate model. *Blood* **115**, 1823–1834.

Rothman, A. L. (2010). Cellular immunology of sequential dengue virus infection and its role in disease pathogenesis. *Curr Top Microbiol Immunol* **338**, 83–98.

Scherer, W. F., Breakenridge, F. A. & Dickerman, R. W. (1972). Cross-protection studies and search for subclinical disease in New World monkeys infected sequentially with different immunologic types of dengue viruses. *Am J Epidemiol* **95**, 67–79.

Scherer, W. F., Russell, P. K., Rosen, L., Casals, J. & Dickerman, R. W. (1978). Experimental infection of chimpanzees with dengue viruses. *Am J Trop Med Hyg* **27**, 590–599.

Schiavetta, A. M., Harre, J. G., Wagner, E., Simmons, M. & Raviprakash, K. (2003). Variable susceptibility of the owl monkey (*Aotus nancymae*) to four serotypes of dengue virus. *Contemp Top Lab Anim Sci* **42**, 12–20.

Shresta, S., Sharar, K. L., Prigozhin, D. M., Beatty, P. R. & Harris, E. (2006). Murine model for dengue virus-induced lethal disease with increased vascular permeability. *J Virol* **80**, 10208–10217.

Styer, L. M., Kent, K. A., Albright, R. G., Bennett, C. J., Kramer, L. D. & Bernard, K. A. (2007). Mosquitoes inoculate high doses of West Nile virus as they probe and feed on live hosts. *PLoS Pathog* **3**, 1262–1270.

Tan, G. K., Ng, J. K., Trasti, S. L., Schul, W., Yip, G. & Alonso, S. (2010). A non mouse-adapted dengue virus strain as a new model of severe dengue infection in AG129 mice. *PLoS Negl Trop Dis* **4**, e672.

Vaughn, D. W., Whitehead, S. S. & Durbin, A. (2008). Viral vaccines. In *Vaccines for Biodefense and Emerging and Neglected Diseases*, pp. 302–304. Edited by A. D. T. Barrett & L. R. Stanberry. London: Academic Press, Elsevier.

Weiskopf, D., Yauch, L. E., Angelo, M. A., John, D. V., Greenbaum, J. A., Sidney, J., Kolla, R. V., De Silva, A. D., de Silva, A. M. & other authors (2011). Insights into HLA-restricted T cell responses in a novel mouse model of dengue virus infection point toward new implications for vaccine design. *J Immunol* **187**, 4268–4279.

Whitehead, R. H., Chaicumpa, V., Olson, L. C. & Russell, P. K. (1970). Sequential dengue virus infections in the white-handed gibbon (*Hylobates lar*). *Am J Trop Med Hyg* **19**, 94–102.

WHO (2009). Dengue: guidelines for diagnosis, treatment, prevention and control. http://whqlibdoc.who.int/publications/2009/9789241547871_eng.pdf.

Xu, M., Hadinoto, V., Appanna, R., Joensson, K., Toh, Y. X., Balakrishnan, T., Ong, S. H., Warter, L., Leo, Y. S. & other authors (2012). Plasmablasts generated during repeated dengue infection are virus glycoprotein-specific and bind to multiple virus serotypes. *J Immunol* **189**, 5877–5885.

Zompi, S. & Harris, E. (2012). Animal models of dengue virus infection. *Viruses* **4**, 62–82.

Zompi, S. & Harris, E. (2013). Original antigenic sin in dengue revisited. *Proc Natl Acad Sci U S A* **110**, 8761–8762.

Zompi, S., Montoya, M., Pohl, M. O., Balmaseda, A. & Harris, E. (2012). Dominant cross-reactive B cell response during secondary acute dengue virus infection in humans. *PLoS Negl Trop Dis* **6**, e1568.

Immunology Letters 154 (2013) 12–17

Contents lists available at ScienceDirect

Immunology Letters

journal homepage: www.elsevier.com/locate/immlet

Efficient *in vivo* depletion of CD8$^+$ T lymphocytes in common marmosets by novel CD8 monoclonal antibody administration

Tomoyuki Yoshida[a,b,*,1], Saori Suzuki[b,1], Yuki Iwasaki[a], Akihisa Kaneko[b], Akatsuki Saito[b], Yuki Enomoto[b], Atsunori Higashino[b], Akino Watanabe[b], Juri Suzuki[b], Kenichi Inoue[b], Teiko Kuroda[b], Masahiko Takada[b], Ryoji Ito[c], Mamoru Ito[c], Hirofumi Akari[a,b,*]

[a] *Tsukuba Primate Research Center, National Institute of Biomedical Innovation, Hachimandai, Tsukuba, Ibaraki 305-0843, Japan*
[b] *Primate Research Institute, Kyoto University, Inuyama, Aichi 484-8506, Japan*
[c] *Central Institute for Experimental Animals, Tomomachi, Kawasaki 210-0821, Japan*

ARTICLE INFO

Article history:
Received 16 April 2013
Received in revised form 4 August 2013
Accepted 12 August 2013
Available online xxx

Keywords:
Monoclonal antibody
CD8 T lymphocyte
Common marmoset
In vivo depletion

ABSTRACT

In order to directly demonstrate the roles of CD8$^+$ T lymphocytes in non-human primates, *in vivo* depletion of the CD8$^+$ T cells by administration of a CD8-specific monoclonal antibody (mAb) is one of the crucial techniques. Recently, the common marmoset (*Callithrix jacchus*), which is classified as a New World monkey, has been shown useful as an experimental animal model for various human diseases such as multiple sclerosis, Parkinson's disease and a number of infectious diseases. Here we show that an anti-marmoset CD8 mAb 6F10, which we have recently established, efficiently depletes the marmoset CD8$^+$ T lymphocytes *in vivo*, *i.e.*, the administration of 6F10 induces drastic and specific reduction in the ratio of the CD8$^+$ T cell subset for at least three weeks or longer. Our finding will help understand the pivotal role of CD8$^+$ T cells *in vivo* in the control of human diseases.

1. Introduction

The use of non-human primates as experimental animal models is highly effective for research on human diseases. Non-human primates and humans share comparable immune systems as compared with mice and are suitable for the evaluation of innate and adaptive immune responses against several viruses [1,2]. On the other hand, there are also several issues with chimpanzees and macaques. The most prevalent being that the use of the chimpanzee is limited by ethical and financial restrictions [3–6].

A New World monkey, the common marmoset (*Callithrix jacchus*) has several advantages as an experimental animal model. The small size of the marmoset makes it easier to handle and reduces maintenance costs [7]. Recently, it has been reported that the marmoset model is a very useful tool in investigating multiple sclerosis (MS), rheumatoid arthritis (RA) and Parkinson's disease [8–10]. Moreover, the marmoset has an immune system similar to that of humans and is suitable for the evaluation of innate and adaptive immune responses against several viruses which efficiently replicate in the marmoset [11–14].

CD8$^+$ T lymphocytes are a vital component of the adaptive immune response and are crucial to the control and clearance of intracellular pathogens. These cells play critical roles in purging acute infections, limiting persistent infections, and conferring lifelong protective immunity. In order to clarify the pivotal role of CD8$^+$ T cells in a variety of non-human primate models for human diseases, *in vivo* depletion of CD8$^+$ T cells by administration of a CD8-specific monoclonal antibody (mAb) is a straightforward technique, although it has been established in Old World monkeys but not in New World monkeys [15–21].

We recently established a novel mAb 6F10 specific for common marmoset CD8 [7]. In this study, we demonstrated for the first time in New World monkeys that the administration of the 6F10 mAb efficiently depleted CD8$^+$ T lymphocytes in marmosets.

2. Materials and methods

2.1. Animals

All animal studies were conducted in accordance with the protocols of experimental procedures that were approved by the Animal Welfare and Animal Care Committee of the Primate Research Institute of Kyoto University, Inuyama, Japan. A total of

* Corresponding authors at: Primate Research Institute, Kyoto University, Inuyama, Aichi 484-8506, Japan. Tel.: +81 568 63 0440; fax: +81 568 62 9559.
E-mail addresses: yoshida.tomoyuki.4w@kyoto-u.ac.jp (T. Yoshida), akari.hirofumi.5z@kyoto-u.ac.jp (H. Akari).
[1] These two authors contributed equally to this work.

0165-2478/$ – see front matter © 2013 Elsevier B.V. All rights reserved.
http://dx.doi.org/10.1016/j.imlet.2013.08.005

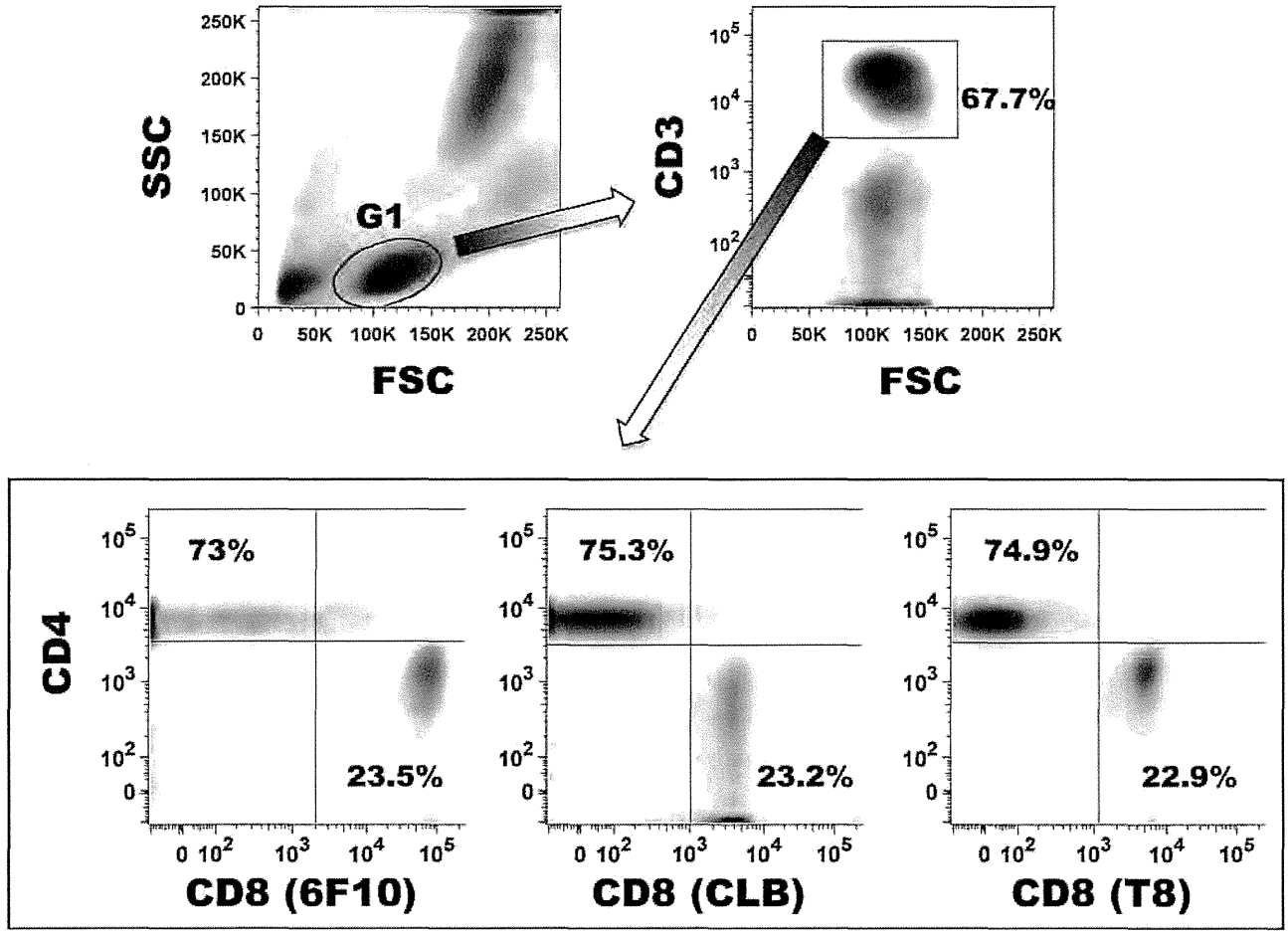

Fig. 1. Flow cytometric analyses of CD3, CD4 and CD8 expression on lymphocytes in marmosets. Fifty microliters of whole blood specimens from marmosets were stained with APC-Cy7-conjugated anti-CD3, PerCP-Cy5.5-conjugated anti-CD4 and APC-conjugated 6F10 mAbs or PE-conjugated CD8 (CLB or T8) mAb. Then, erythrocytes were lyzed and the stained cells were resuspended in the fix buffer. Representative results in a marmoset are shown. The G1 lymphocyte population was selected (left top panel) and a $CD3^+$ T cell subset was gated (right top panel). Fluorescence intensity for CD4 and CD8 in the T cell subset was depicted (lower panels).

three marmosets, weighing 357–457 g, were used. Common marmosets were caged individually at 27 ± 2 °C in 50 ± 10% humidity with a 12 h light–dark cycle (lighting from 7:00 to 19:00) in our facility. All animals were fed twice a day with a standard marmoset diet supplemented with fruit and mealworm. Water was given *ad libitum*.

2.2. Flow cytometry

Flow cytometry was performed as previously described with a slight modification [22]. A previously established mouse anti-marmoset CD8 mAb named 6F10 was used [7]. The 6F10 mAb was conjugated with allophycocyanin (APC) and by Zenon Mouse IgG labeling Kit (Molecular Probes) according to the manufacturer's instruction. Fifty microliters of whole blood from marmosets was stained with combinations of fluorescence-conjugated mAb: APC-Cy7-conjugated anti-CD3 (SP34-2: Becton Dickinson), PerCP-Cy5.5-conjugated anti-CD4 (L200: BD Pharmingen), PE-conjugated anti-CD8 (CLB-T8/4, 4H8 (CLB hereafter): Sanquin; RPA-T8 (T8 hereafter): Becton Dickinson) and FITC-conjugated anti-CD20 (H299: BECKMAN COULTER). Then, erythrocytes were lyzed with FACS lyzing solution (Becton Dickinson). After washing with a sample buffer containing phosphate-buffered saline (PBS) and 1% fetal calf serum (FCS), the labeled cells were resuspended in a fix buffer containing PBS and 1% formaldehyde. The expression of the immunolabeled molecules on the lymphocytes was analyzed with a FACSCanto II flow cytometer (Becton Dickinson). The data analysis was conducted using FlowJo software (Treestar, Inc.).

2.3. In vitro binding competition of anti-CD8 mAbs

Fifty microliters of whole blood from marmosets was treated with increasing amounts (1, 10, 100 ng) of the 6F10 mAb on ice for 30 min. After washing with the sample buffer, the cells were stained with fluorescence-conjugated mAbs against CD3, CD4, and CD8 on ice for 30 min. Then, erythrocytes were lyzed with FACS lyzing solution (Becton Dickinson). After washing with the sample buffer, the labeled cells were resuspended in the fix buffer. The fluorescence intensity of the cells were analyzed at is as described above.

2.4. In vivo depletion of $CD8^+$ T lymphocytes

In vivo depletion of the marmoset $CD8^+$ T lymphocytes was performed as previously described [19]. Briefly, the 6F10 or a control mAb (MOPC-21) was administrated subcutaneously to the subject at 10 mg/kg (body weight) followed by intravenous administration at 5 mg/kg in the saphenous vein at a rate of 20 ml/h using a syringe pump on days 3, 7, 10 after the primary administration. The kinetics for the percentages of $CD8^+$ and $CD4^+$ cells in a $CD3^+$ T cell subset as well as the percentages of $CD20^+$ B cells and $CD3^-CD20^-$ cells in the

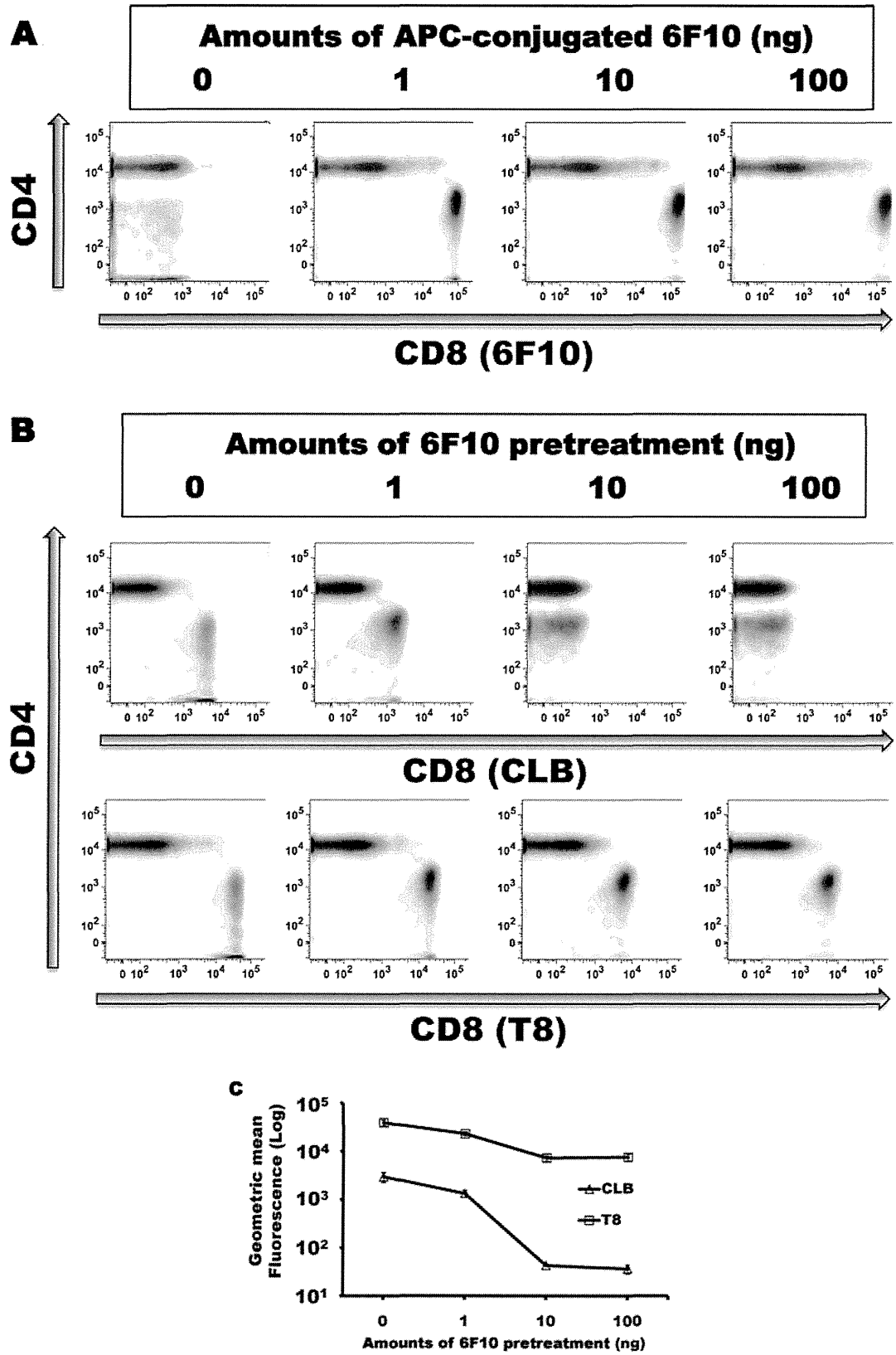

Fig. 2. Binding competition among anti-CD8 mAbs in marmoset CD8$^+$ T cells. (A) Fifty microliters of whole blood specimens from marmosets were stained with APC-Cy7-conjugated CD3 and PerCP-Cy5.5-conjugated CD4 mAbs and increasing amounts (1, 10, 100 ng) of APC-conjugated 6F10 mAb. Then, erythrocytes were lyzed and the stained cells were resuspended in the fix buffer. The fluorescence intensity for CD4$^+$ and CD8$^+$ cells in a CD3$^+$ T cell subset was shown. (B and C) Fifty microliters of whole blood specimens were pretreated with increasing amounts (1, 10, 100 ng) of 6F10 mAb, followed by staining with fluorescence-conjugated mAbs against CD3, CD4, and CD8 (CLB or T8). Fluorescence intensity of CD4$^+$ and CD8$^+$ cells in a CD3$^+$ T cell subset was shown (B) and the geometric mean fluorescence of CD8$^+$ T cells labeled by the CLB or T8 mAbs was indicated. We analyzed statistically whether geometric means were different in each antibody by using StatView software.

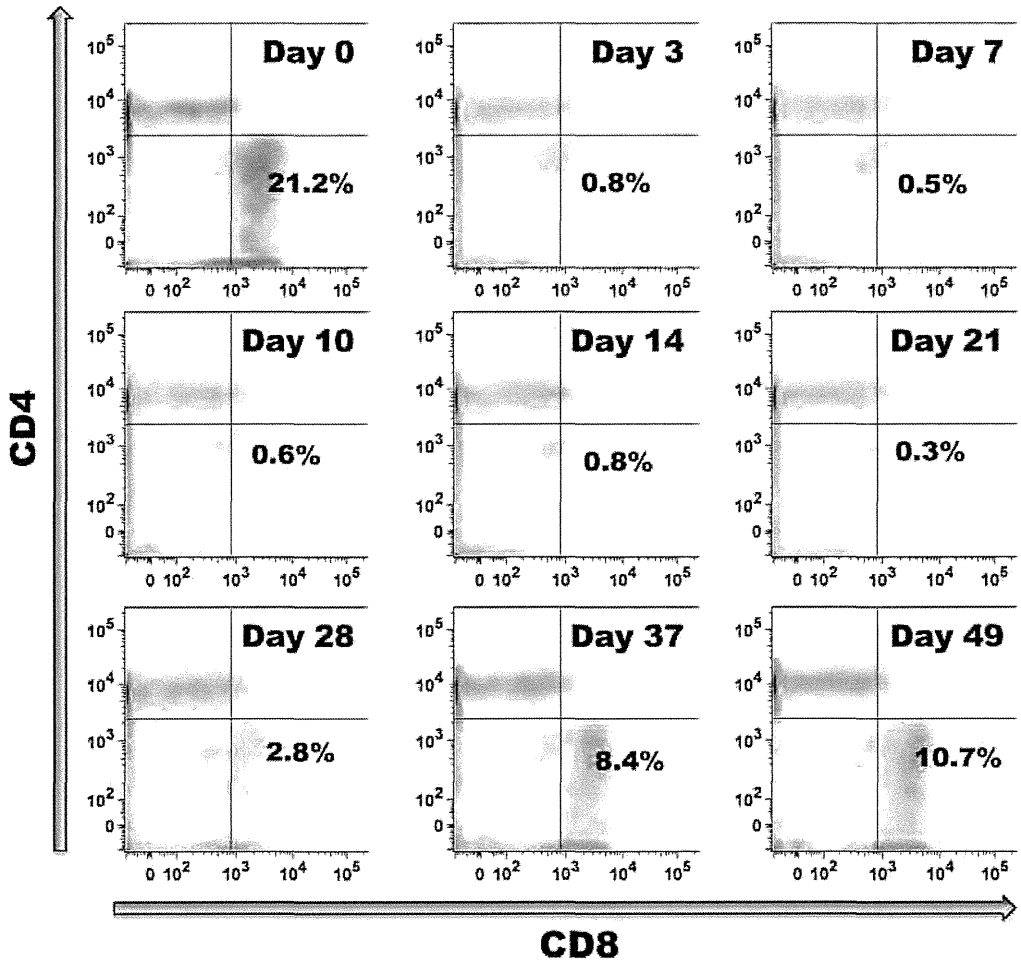

Fig. 3. *In vivo* depletion of CD8$^+$ T cells by administration of a marmoset anti-CD8 mAb 6F10. Periodical kinetics for the fluorescence intensity of CD4$^+$ and CD8$^+$ cells in a CD3$^+$ T cell subset of Cj175 administered subcutaneously with 10 mg/kg of the 6F10 mAb, followed by 5 mg/kg administration intravenously at days 3, 7, and 10 were shown.

total lymphocytes of each marmoset were periodically monitored during the observation period as indicated.

2.5. Statistical analyses

Statistical analyses of lymphocyte ratios were performed using Student's *t*-test and single-factor ANOVA, followed by Fisher's protected least-significant difference *post hoc* test by using StatView software (SAS Institute, NC, USA).

3. Results

3.1. Lymphocyte subsets in marmosets

We previously demonstrated that the 6F10 mAb specifically detected CD8$^+$ T lymphocytes in marmosets by using flow cytometry as well as immunohistochemical and Western blot analyses [7]. Basic information regarding CD4/CD8 naïve and central/effector memory T cells and NK/NKT cells in marmosets was available from our recent report [13]. We compared the immunoreactivity of the 6F10 mAb with other commercially available CD8 mAbs in lymphocyte subsets of marmosets (Fig. 1). The gating strategy for profiling CD4$^+$ and CD8$^+$ T cells was shown in Fig. 1. The percentage of CD8$^+$ T cells in a CD3$^+$ T cell subset as detected by 6F10, CLB or T8 anti-CD8 mAb was comparable (23.5%, 23.2% and 22.9%, respectively). Notably, the 6F10 mAb poorly cross-reacted with tamarin and rhesus macaque CD8$^+$ T cells while CLB and T8 mAbs did with both (data not shown). It is reasonable that the 6F10 mAb showed selected specificity to the marmoset CD8, considering that it was established by immunization with marmoset lymphocytes [7].

3.2. In vitro binding competition of anti-CD8 antibodies in CD8$^+$ T cells of marmosets

We initially treated the marmoset lymphocytes with increasing amounts of APC-conjugated 6F10 together with fluorescence-labeled mAbs to CD3 and CD4. It was found that fluorescence intensity for APC on a CD3$^+$ T cell subset was saturated by 10 ng or more of 6F10 mAb (Fig. 2A). We then sought to define whether the binding epitope of 6F10 mAb in the marmoset CD8 molecule was overlapped with the epitopes of T8 and CLB mAbs by a competition assay. It was found that fluorescence intensity in the CD3$^+$ T cell subset treated with the labeled CLB mAb was drastically reduced by the pretreatment of 10 or 100 ng 6F10 (Fig. 2B and C). On the other hand, the 6F10 pretreatment scarcely influenced fluorescence intensity in the cells that reacted with the labeled T8 mAb, irrespective of the amounts of 6F10 (Fig. 2B and C). These results indicated that 6F10 competitively inhibited binding of CLB but not T8 mAbs to CD8, suggesting that the binding epitope for 6F10 was overlapped with that of CLB and was sterically apart from that of T8. In addition, T8 was likely to exhibit greater affinity than CLB to marmoset CD8 (Fig. 2B).

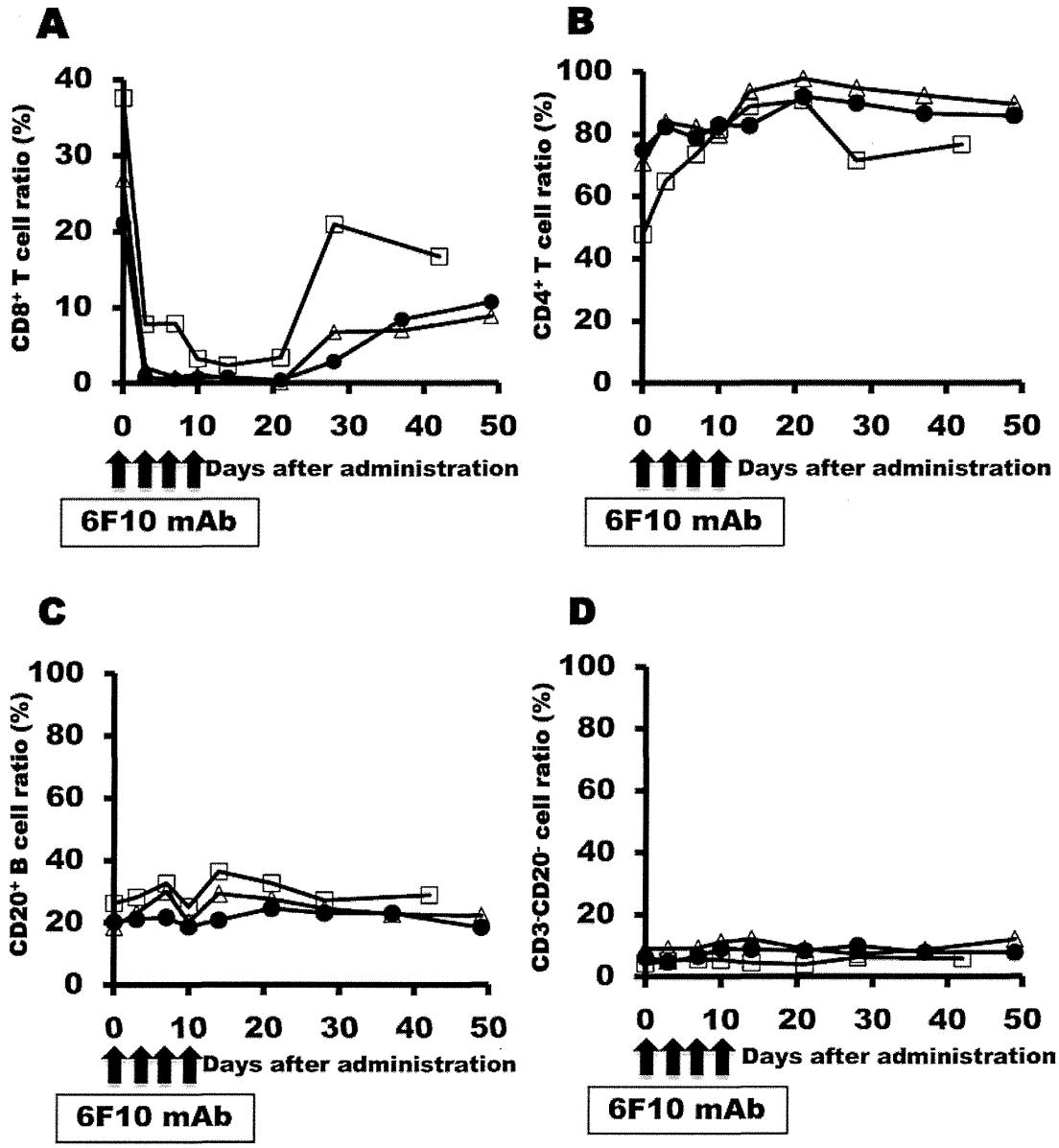

Fig. 4. The kinetics for the ratios of $CD8^+$ cells (A) and $CD4^+$ cells (B) in a $CD3^+$ T cell subset as well as $CD20^+$ B cells (C) and $CD3^-CD20^-$ cells (D) in total lymphocytes of each marmoset after the administration of the 6F10 mAb were shown.

3.3. In vivo depletion of $CD8^+$ T cells using an anti-marmoset CD8 mAb

We finally examined whether the administration of the 6F10 mAb could influence $CD8^+$ T lymphocytes *in vivo*. Three marmosets were subcutaneously administrated at 10 mg/kg followed by intravenous administration at 5 mg/kg on days 3, 7, 10 after the primary administration. The mAb-treated marmosets did not develop any clinical and hematological signs (data not shown). In order to detect $CD8^+$ T lymphocytes in the 6F10-treated marmosets, we employed T8 mAb, which was found to react with CD8 molecule in the presence of 6F10 as shown in Fig. 2. It was found that at 10 days after the mAb administration the $CD8^+$ T cells were almost completely depleted, followed by gradual recovery to a half of the initial levels at around 4–7 weeks later (Fig. 3). It is noteworthy that the treatment relatively increased in the proportion of $CD4^+$ T cells in compensation for the depletion of $CD8^+$ T cells, while the ratios of $CD20^+$ B cells and $CD3^-CD20^-$ cells were scarcely affected (Fig. 4). In addition, administration of a control antibody (MOPC-21) did not affect any lymphocyte subsets (data not shown). These results demonstrated that the 6F10 mAb was able to specifically deplete $CD8^+$ T cells in marmosets.

4. Discussion

In this study, we attempted to establish a technical basis for the study of $CD8^+$ T cells in marmosets. We assessed the effect of a 6F10 mAb administration *in vivo* and found that $CD8^+$ T cells were efficiently depleted in the blood of the treated monkeys for at least three weeks or longer and that in compensation for the depletion proportion of $CD4^+$ T cells were relatively increased without obvious influence on other lymphocyte subsets such as $CD20^+$ B cells and $CD3^-CD20^-$ cells. This is the first report showing the establishment of new methodology to deplete common marmoset $CD8^+$ T lymphocytes *in vivo*. Since demand for marmosets as non-human primate models for a variety of inflammatory and autoimmune diseases as well as infectious diseases has been increasing, our findings will provide new techniques to scientists who are eager to examine

the pivotal role of $CD8^+$ T lymphocytes *in vivo* in the onset of the human diseases.

We previously sought to examine the dynamics of cellular immune responses in the acute phase of dengue virus (DENV) infection in a novel marmoset model that we recently developed [12]. We found that the DENV infection in marmosets greatly induced early immune responses of CD4/CD8 central memory T cells, suggesting that the cellular immunity may be associated with the control of primary DENV infection [13]. Considering this, the present techniques to deplete $CD8^+$ T cells *in vivo* will provide a useful tool to further elucidate the functional role of $CD8^+$ T cells in the acute DENV infection.

Common marmosets are suitable for detailed observations of the movement of the extremities and cognitive functions, which approximate those of humans. Therefore, marmosets are highly useful as models of neurological diseases such as Parkinson's, MS and RA. Importantly, the marmoset models for analyzing Parkinson's disease and autoimmune diseases such as MS and RA have already been developed [8–10,23]. $CD8^+$ T cells have been implicated in the pathogenesis of autoimmune disorders including diseases of the central nervous system such as MS, encephalomyelitis and diabetes mellitus [24–26]. MS is an immune-mediated disease of the central nervous system leading to demyelination and axonal/neuronal loss. Accumulating evidence points to a key role for $CD8^+$ T cells in the disease; histopathological analyses and compelling observations from animal models indicate that cytotoxic $CD8^+$ T cells target neural cell populations with the potential of causing lesions consistent with MS [27]. RA is a systemic and chronic autoimmune disease characterized mainly by synovial inflammation leading to joint destruction and disability with a huge impact upon the quality of life and life expectancy. Several studies have demonstrated that $CD8^+$ T cells in RA have powerful cytotoxic ability and therefore exhibit the potential to enhance the disease [28]. Thus, our *in vivo* CD8 depletion technics will be valuable in further examining the role of $CD8^+$ T cells in these autoimmune diseases in the marmoset models.

Conflict of interest statement

None declared.

Acknowledgments

We would like to give special thanks to members of Corporation for Production and Research of Laboratory Primates and Center for Human Evolution Modeling Research, Primate Research Institute of Kyoto University for technical assistance. We also would like to give special thanks to Ms. Atsuko Owashi and Yumiko Hasegawa for technical assistance. This work was supported by grants from the Ministry of Health, Labor and Welfare of Japan and Ministry of Education, Culture, Sports, Science and Technology of Japan.

References

[1] Meuleman P, Leroux-Roels G. HCV animal models: a journey of more than 30 years. Viruses 2009;1:222–40.
[2] Zompi S, Harris E. Animal models of dengue virus infection. Viruses 2012;4:62–82.
[3] Gagneux P, Moore JJ, Varki A. The ethics of research on great apes. Nature 2005;437:27–9.
[4] Knight A. The beginning of the end for chimpanzee experiments? Philos Ethics Humanit Med 2008;3:16.
[5] Morimura N, Idani G, Matsuzawa T. The first chimpanzee sanctuary in Japan: an attempt to care for the "surplus" of biomedical research. Am J Primatol 2011;73:226–32.
[6] Brass V, Moradpour D, Blum HE. Hepatitis C virus infection: in vivo and in vitro models. J Viral Hepat 2007;14(Suppl. 1):64–7.
[7] Ito R, Maekawa S, Kawai K, Suemizu H, Suzuki S, Ishii H, et al. Novel monoclonal antibodies recognizing different subsets of lymphocytes from the common marmoset (*Callithrix jacchus*). Immunol Lett 2008;121:116–22.
[8] Ando K, Obayashi S, Nagai Y, Oh-Nishi A, Minamimoto T, Higuchi M, et al. PET analysis of dopaminergic neurodegeneration in relation to immobility in the MPTP-treated common marmoset, a model for Parkinson's disease. PLoS ONE 2012;7:e46371.
[9] Jagessar SA, Gran B, Heijmans N, Bauer J, Laman JD, t Hart BA, et al. Discrepant effects of human interferon-gamma on clinical and immunological disease parameters in a novel marmoset model for multiple sclerosis. J Neuroimmune Pharmacol 2012;7:253–65.
[10] Petersen F, Yu X. A novel preclinical model for rheumatoid arthritis research. Arthritis Res Ther 2010;12:148.
[11] Woollard DJ, Haqshenas G, Dong X, Pratt BF, Kent SJ, Gowans EJ. Virus-specific T-cell immunity correlates with control of GB virus B infection in marmosets. J Virol 2008;82:3054–60.
[12] Omatsu T, Moi ML, Hirayama T, Takasaki T, Nakamura S, Tajima S, et al. Common marmoset (*Callithrix jacchus*) as a primate model of dengue virus infection: development of high levels of viraemia and demonstration of protective immunity. J Gen Virol 2011;92:2272–80.
[13] Yoshida T, Omatsu T, Saito A, Katakai Y, Iwasaki Y, Kurosawa T, et al. Dynamics of cellular immune responses in the acute phase of dengue virus infection. Arch Virol 2013;158:1209–20.
[14] Omatsu T, Moi ML, Takasaki T, Nakamura S, Katakai Y, Tajima S, et al. Changes in hematological and serum biochemical parameters in common marmosets (*Callithrix jacchus*) after inoculation with dengue virus. J Med Primatol 2012;41:289–96.
[15] Barry AP, Silvestri G, Safrit JT, Sumpter B, Kozyr N, McClure HM, et al. Depletion of CD8+ cells in sooty mangabey monkeys naturally infected with simian immunodeficiency virus reveals limited role for immune control of virus replication in a natural host species. J Immunol 2007;178:8002–12.
[16] Castro BA, Homsy J, Lennette E, Murthy KK, Eichberg JW, Levy JA. HIV-1 expression in chimpanzees can be activated by CD8+ cell depletion or CMV infection. Clin Immunol Immunopathol 1992;65:227–33.
[17] Ramalingam RK, Meyer-Olson D, Shoukry NH, Bowen DG, Walker CM, Kalams SA. Kinetic analysis by real-time PCR of hepatitis C virus (HCV)-specific T cells in peripheral blood and liver after challenge with HCV. J Virol 2008;82:10487–92.
[18] Shoukry NH, Grakoui A, Houghton M, Chien DY, Ghrayeb J, Reimann KA, et al. Memory CD8+ T cells are required for protection from persistent hepatitis C virus infection. J Exp Med 2003;197:1645–55.
[19] Saito A, Nomaguchi M, Iijima S, Kuroishi A, Yoshida T, Lee YJ, et al. Improved capacity of a monkey-tropic HIV-1 derivative to replicate in cynomolgus monkeys with minimal modifications. Microbes Infect 2011;13:58–64.
[20] Jin X, Bauer DE, Tuttleton SE, Lewin S, Gettie A, Blanchard J, et al. Dramatic rise in plasma viremia after CD8(+) T cell depletion in simian immunodeficiency virus-infected macaques. J Exp Med 1999;189:991–8.
[21] Metzner KJ, Jin X, Lee FV, Gettie A, Bauer DE, Di Mascio M, et al. Effects of in vivo CD8(+) T cell depletion on virus replication in rhesus macaques immunized with a live, attenuated simian immunodeficiency virus vaccine. J Exp Med 2000;191:1921–31.
[22] Yoshida T, Saito A, Iwasaki Y, Iijima S, Kurosawa T, Katakai Y, et al. Characterization of natural killer cells in tamarins: a technical basis for studies of innate immunity. Front Microbiol 2010;1:128.
[23] Jagessar SA, Heijmans N, Bauer J, Blezer EL, Laman JD, Hellings N, et al. B-cell depletion abrogates T cell-mediated demyelination in an antibody-nondependent common marmoset experimental autoimmune encephalomyelitis model. J Neuropathol Exp Neurol 2012;71:716–28.
[24] Annibali V, Ristori G, Angelini DF, Serafini B, Mechelli R, Cannoni S, et al. CD161(high)CD8+ T cells bear pathogenetic potential in multiple sclerosis. Brain 2011;134:542–54.
[25] York NR, Mendoza JP, Ortega SB, Benagh A, Tyler AF, Firan M, et al. Immune regulatory CNS-reactive CD8+ T cells in experimental autoimmune encephalomyelitis. J Autoimmun 2010;35:33–44.
[26] Wang J, Ma Y, Knechtle SJ. Adenovirus-mediated gene transfer into rat cardiac allografts. Comparison of direct injection and perfusion. Transplantation 1996;61:1726–9.
[27] Saxena A, Martin-Blondel G, Mars LT, Liblau RS. Role of CD8 T cell subsets in the pathogenesis of multiple sclerosis. FEBS Lett 2011;585:3758–63.
[28] Carvalheiro H, da Silva JA, Souto-Carneiro MM. Potential roles for CD8(+) T cells in rheumatoid arthritis. Autoimmun Rev 2013;12:401–9.

Miura et al. Retrovirology 2013, 10:118
http://www.retrovirology.com/content/10/1/118

RETROVIROLOGY

RESEARCH Open Access

Characterization of simian T-cell leukemia virus type 1 in naturally infected Japanese macaques as a model of HTLV-1 infection

Michi Miura[1], Jun-ichiro Yasunaga[1], Junko Tanabe[1], Kenji Sugata[1], Tiejun Zhao[1,4], Guangyong Ma[1], Paola Miyazato[1], Koichi Ohshima[2], Akihisa Kaneko[3], Akino Watanabe[3], Akatsuki Saito[3], Hirofumi Akari[3] and Masao Matsuoka[1*]

Abstract

Background: Human T-cell leukemia virus type 1 (HTLV-1) causes chronic infection leading to development of adult T-cell leukemia (ATL) and inflammatory diseases. Non-human primates infected with simian T-cell leukemia virus type 1 (STLV-1) are considered to constitute a suitable animal model for HTLV-1 research. However, the function of the regulatory and accessory genes of STLV-1 has not been analyzed in detail. In this study, STLV-1 in naturally infected Japanese macaques was analyzed.

Results: We identified spliced transcripts of STLV-1 corresponding to HTLV-1 *tax* and HTLV-1 bZIP factor (*HBZ*). STLV-1 Tax activated the NFAT, AP-1 and NF-κB signaling pathways, whereas STLV-1 bZIP factor (SBZ) suppressed them. Conversely, SBZ enhanced TGF-β signaling and induced Foxp3 expression. Furthermore, STLV-1 Tax activated the canonical Wnt pathway while SBZ suppressed it. STLV-1 Tax enhanced the viral promoter activity while SBZ suppressed its activation. Then we addressed the clonal proliferation of STLV-1$^+$ cells by massively sequencing the provirus integration sites. Some clones proliferated distinctively in monkeys with higher STLV-1 proviral loads. Notably, one of the monkeys surveyed in this study developed T-cell lymphoma in the brain; STLV-1 provirus was integrated in the lymphoma cell genome. When anti-CCR4 antibody, mogamulizumab, was administered into STLV-1-infected monkeys, the proviral load decreased dramatically within 2 weeks. We observed that some abundant clones recovered after discontinuation of mogamulizumab administration.

Conclusions: STLV-1 Tax and SBZ have functions similar to those of their counterparts in HTLV-1. This study demonstrates that Japanese macaques naturally infected with STLV-1 resemble HTLV-1 carriers and are a suitable model for the investigation of persistent HTLV-1 infection and asymptomatic HTLV-1 carrier state. Using these animals, we verified that mogamulizumab, which is currently used as a drug for relapsed ATL, is also effective in reducing the proviral load in asymptomatic individuals.

Keywords: Simian T-cell leukemia virus, Human T-cell leukemia virus, Tax, HBZ

Background

Human T-cell leukemia virus type 1 (HTLV-1) was the first human retrovirus found to cause a neoplastic disease, adult T-cell leukemia (ATL) [1,2]. Approximately 10 million people worldwide are estimated to be infected with this virus. HTLV-1 is endemic in specific areas including south-western Japan, Central and South America, the Caribbean, and intertropical Africa [3]. Most HTLV-1 carriers remain asymptomatic through their lives and only a small fraction of them develop ATL, a leukemia of HTLV-1-infected CD4$^+$ T cells, after a long latent period [4]. This virus also causes inflammatory disorders such as HTLV-1-associated myelopathy/tropic spastic paraparesis (HAM/TSP) [5,6] and uveitis [7].

The reason why most HTLV-1 carriers do not develop ATL is partly explained by the immune response of cytotoxic T cells (CTLs) against HTLV-1 proteins [8]. Immunosuppressive conditions, particularly following organ or bone

* Correspondence: mmatsuok@virus.kyoto-u.ac.jp
[1]Laboratory of Virus Control, Institute for Virus Research, Kyoto University, Shogoin Kawahara-cho 53, Sakyo-ku, Kyoto 606-8507, Japan
Full list of author information is available at the end of the article

marrow transplantation, can induce the development of ATL [9,10], indicating that the host immune system usually prevents the development of ATL. Two HTLV-1 proteins, Tax and HTLV-1 bZIP factor (HBZ), are thought to promote the proliferation of infected cells and ATL cells [4,11]. Tax is highly immunogenic to CTLs and the infected cells expressing Tax are kept to a small number [12]. Recently, it has been reported that CTLs to HBZ play a critical role in determining proviral load in carriers [13].

Animal models that are relevant to the human immune system are required for scientists to investigate how the immune response controls the proliferation of infected cells and viral replication *in vivo*. Old World monkeys are frequently infected with simian T-cell leukemia virus type 1 (STLV-1), which is closely related to HTLV-1 [14]. Like HTLV-1 infection, clonal proliferation of STLV-1-infected cells was detected by inverse PCR [15]. Furthermore, STLV-1 also leads to the development of lymphoproliferative diseases [16,17]. Based on these observations, it has been proposed that STLV-1-infected non-human primates may constitute a suitable animal model for HTLV-1 research. However, a detailed characterization of STLV-1 infection in non-human primates has not been achieved.

In the present study, Japanese macaques naturally infected with STLV-1 were investigated. We first identified the STLV-1 bZIP factor (SBZ) gene as an antisense transcript of STLV-1 similar to HBZ. Molecular analyses showed that STLV-1 Tax and SBZ have activities on various transcriptional pathways similar to those of HTLV-1 Tax and HBZ. Furthermore, we observed clonal proliferation of STLV-1-infected cells. Finally, anti-CCR4 antibody, which is currently used to treat ATL patients, was administered into STLV-1-infected Japanese macaques, and we found that this reduced the proviral load *in vivo*, indicating that anti-CCR4 antibody is effective for treatment of HTLV-1-associated inflammatory diseases. These results suggest that Japanese macaques naturally infected with STLV-1 show characteristics that correlate closely with those of HTLV-1 carriers and may therefore serve as a suitable animal model for the analysis of persistent HTLV-1 infection and HTLV-1 carrier state.

Results

Seroprevalence and proviral load of STLV-1 in Japanese macaques

To identify STLV-1-infected monkeys, we screened plasma samples for antibody against viral STLV-1 antigens by particle-agglutination test. Out of 533 Japanese macaques examined, 320 (60%) were seropositive, while only one rhesus macaque out of 163 (0.6%) was seropositive (Figure 1A). Proviral load in white blood cells was measured by quantitative real-time PCR for 115 seropositive Japanese macaques. Proviral load ranged from 0.001% to over 10% (Figure 1B). Since the DNA samples used in the above experiment were obtained from total white blood cells including granulocytes, these data likely underestimate proviral load of PBMCs.

Functional similarity of STLV-1 Tax and STLV-1 bZIP factor to their counterparts in HTLV-1

Analysis of the STLV-1 pX region suggests the presence of *tax* coding gene and an antisense transcript in the minus strand of STLV-1 similar to *HBZ*. In order to examine if STLV-1 *tax* and *SBZ* genes are transcribed and processed to be mature mRNAs in STLV-1-infected PBMCs, STLV-1 *tax* and *SBZ* transcripts were amplified by RT-PCR using the primers flanking the putative splicing site (Figure 2). The length of the amplified fragments was comparable to that of the corresponding HTLV-1 transcripts, which are approximately 240 bp for *tax* and 310 bp for *HBZ*. We further verified that STLV-1 *tax* and *SBZ* transcripts are spliced at exactly the same location as HTLV-1 *tax* and spliced form of *HBZ* [11,18], respectively (Figure 2). To investigate the molecular functions of STLV-1 Tax and SBZ, we cloned the coding sequences of those proteins from the STLV-1 provirus in a Japanese macaque (Mf-5). Approximately 91% of the coding sequence of *tax* was identical in HTLV-1 (ATK) and Japanese macaque STLV-1, and 82% in *HBZ* (ATK) and Japanese macaque *SBZ*. Phylogenetic analyses show that Japanese macaque STLV-1 *env* in this study is close to Melanesian subtype C [5] (Additional file 1). Therefore, the STLV-1 protein sequences were aligned with HTLV-1 prototype ATK (subtype A) as well as Mel5

A

	Total number of macaques examined	Antibody-positive	Positivity
Japanese macaques	533	320	60%
rhesus macaques	163	1	0.6%

B

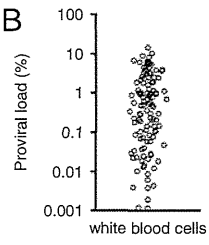

Figure 1 STLV-1 infection in Japanese and rhesus macaques. (A) STLV-1 seropositivity in Japanese macaques and rhesus macaques screened in this study is shown. **(B)** STLV-1 proviral load (percentage) in white blood cells of Japanese macaques is shown.

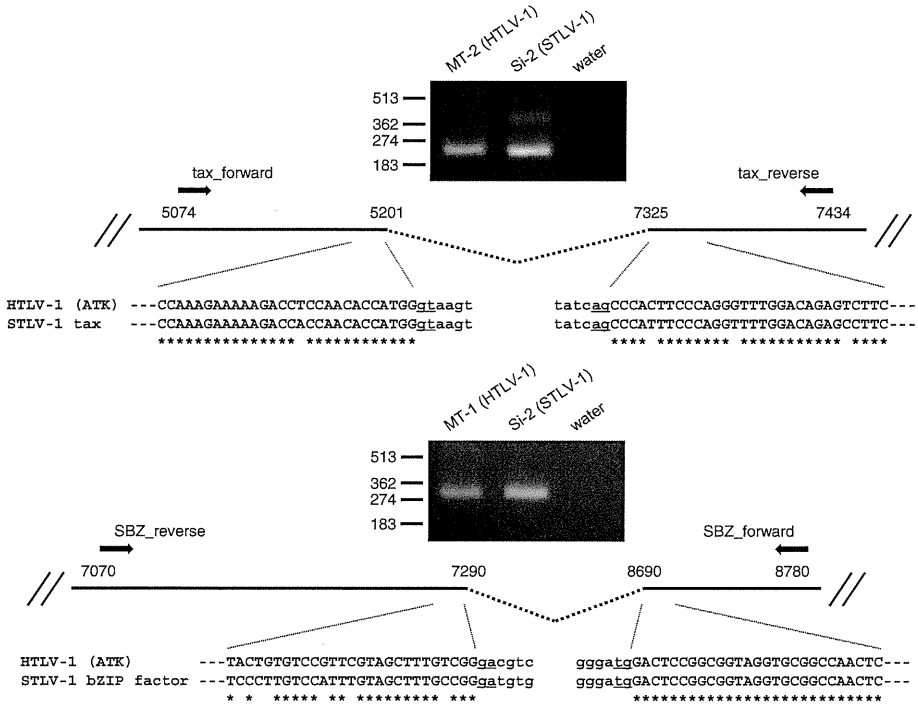

Figure 2 Detection of STLV-1 *tax* and *STLV-1 bZIP factor* (*SBZ*) transcripts and their splicing junctions. STLV-1 *tax* and *SBZ* transcripts were amplified by RT-PCR using the primers flanking the putative splicing site. The bands of the amplified fragments are shown together with the corresponding transcript of HTLV-1 in the images of agarose gel stained with ethidium bromide. Numbers in the scheme indicate the nucleotide positions of HTLV-1 ATK provirus. Sequences of the amplified STLV-1 *tax* and *SBZ* transcripts are represented with uppercase letters and aligned with a reference sequence of HTLV-1 (ATK). The lowercase letters represent the intron region of HTLV-1 or STLV-1 provirus.

(subtype C) for comparison, and presented in Figure 3. Approximately 93% of the STLV-1 Tax amino acid sequence was identical to that of HTLV-1 Tax (Figure 3A) and approximately 73% of the amino acid sequence of SBZ was identical to that of HBZ (Figure 3B). Notably, SBZ has some insertions and deletions, resulting in an excess of three amino acids compared with HBZ.

It was previously shown that HTLV-1 Tax activates the NF-κB, NFAT and AP-1 pathways [19,20], whereas HBZ suppresses them [21]. The effect of STLV-1 Tax on these

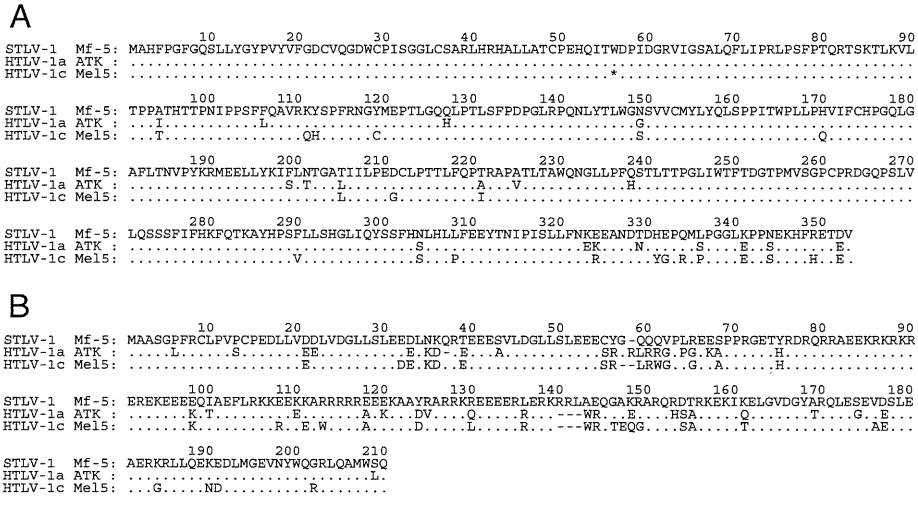

Figure 3 Comparison of the amino acid sequences of STLV-1 Tax and SBZ with those of HTLV-1 Tax and HBZ. Amino acid sequences of STLV-1 Tax **(A)** and SBZ **(B)** derived from an STLV-1$^+$ Japanese macaque (Mf-5) are compared respectively with those of HTLV-1 Tax and HBZ from two isolates. Asterisk represents the termination codon. Accession number: [GenBank:J02029] (ATK) and [GenBank:L02534] (Mel5).

pathways was analyzed using luciferase assays. We found that, like HTLV-1 Tax, STLV-1 Tax activated these pathways (Figure 4A). Conversely, SBZ suppressed these pathways when they were activated by phorbol myristate acetate and ionomycin (NFAT and AP-1) or HTLV-1 Tax (NF-κB) (Figure 4B).

Recently, our group reported that HBZ enhances TGF-β signaling via interaction with Smad2/3 and p300, thus inducing the expression of Foxp3 *in vitro* [22]. The analysis of HBZ transgenic mice further demonstrated an increase in Foxp3$^+$ T cells [23]. Therefore, we investigated whether SBZ also enhances TGF-β signaling. We found that SBZ enhanced signaling by the TGF-β pathway, while STLV-1 Tax suppressed it (Figure 4C). Like HBZ, expression of SBZ in mouse naïve CD4$^+$ T cells induced expression of Foxp3, and this expression was significantly enhanced by TGF-β (Figure 5). Thus, SBZ, like its counterpart HBZ, activates the TGF-β/Smad pathway and induces Foxp3 expression in CD4$^+$ T cells.

Next we studied STLV-1 Tax and SBZ for their capability to regulate the canonical Wnt pathway in the manner we recently reported for HTLV-1 Tax and HBZ [24]. STLV-1 Tax, like HTLV-1 Tax, elevated the activity of luciferase regulated by the promoter responsive to TCF/LEF in the presence of Dvl2 and DAPLE (Figure 4D). In contrast, when SBZ was co-expressed with Tax, luciferase activity was

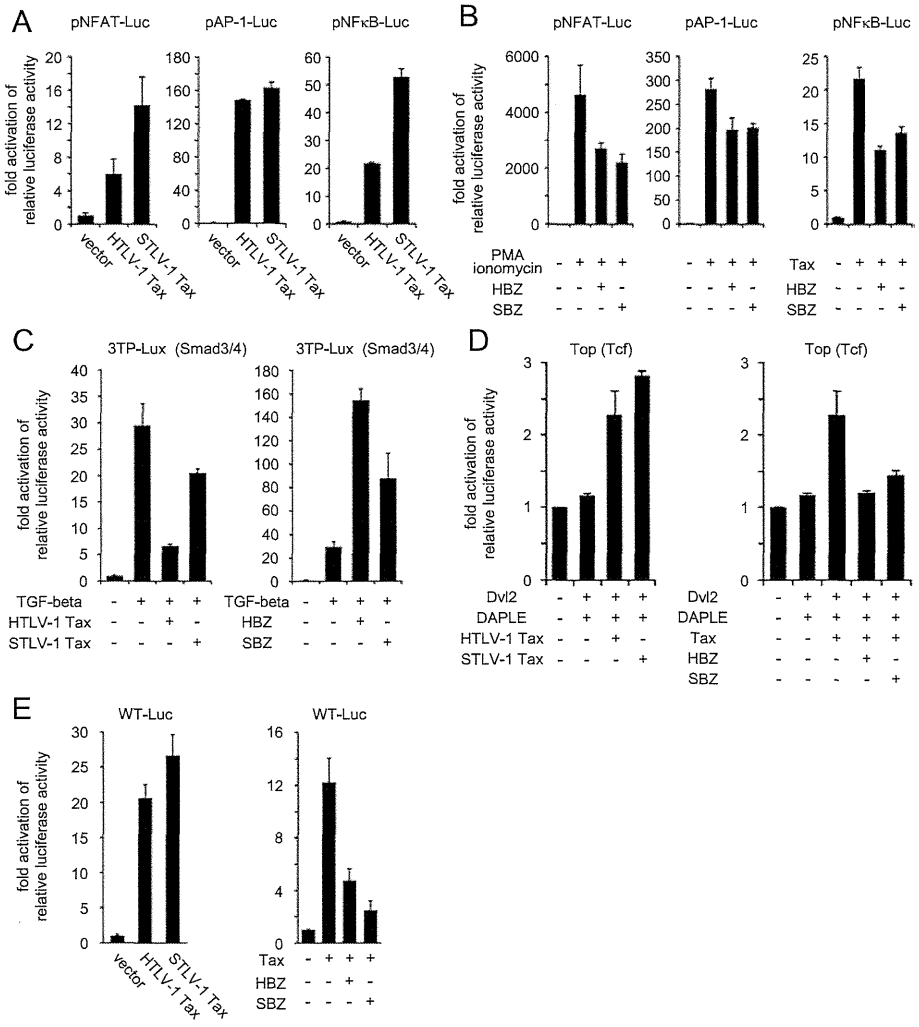

Figure 4 Effects of STLV-1 Tax and SBZ on various signaling pathways. Effects of HTLV-1 Tax or STLV-1 Tax **(A)**, and HBZ or SBZ **(B)** were analyzed using reporter plasmids for the NFAT, AP-1 and NF-κB pathways in Jurkat cells. **(C)** The effects of HTLV-1 Tax or STLV-1 Tax (left) and HBZ or SBZ (right) on the TGF-β signaling pathway were analyzed in HepG2 cells using the reporter plasmid 3TP-Lux, which contains the responsive element to Smad3/4. **(D)** The effects of HTLV-1 Tax or STLV-1 Tax (left) and HBZ or SBZ (right) on relative luciferase activity driven by TCF-responsive elements were analyzed using Jurkat cells. **(E)** The effects of HTLV-1 Tax or STLV-1 Tax (left) and HBZ or SBZ (right) on relative luciferase activity driven by viral LTR were analyzed using Jurkat cells. Firefly luciferase activity was normalized to that of Renilla luciferase and represented as fold activation compared to the relevant control. The data represent mean and standard deviation.

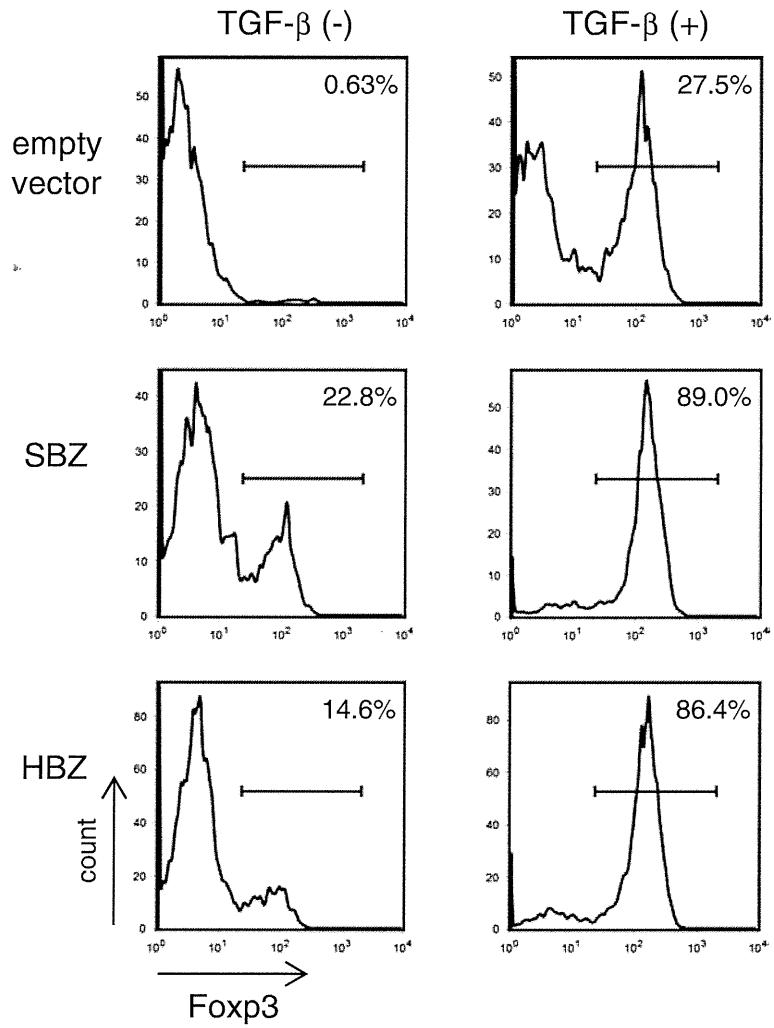

Figure 5 Flow cytometric analyses of Foxp3 induction by SBZ. SBZ or HBZ transduced mouse T cells that were positive for the transduction marker were analyzed for Foxp3 expression. The percentage of cells positive for Foxp3 is shown in each histogram. Each experiment was done at least in triplicate, and representative results are shown.

suppressed (Figure 4D). These results demonstrate that like their counterparts in HTLV-1, STLV-1 Tax activates the canonical Wnt pathway while SBZ suppresses it.

Lastly, regulation of viral promoter activity by STLV-1 Tax and SBZ was examined since it is known that HTLV-1 Tax activates the viral transcription from the 5' long terminal repeat (LTR) of the provirus while HBZ suppresses it. As presented in Figure 4E, STLV-1 Tax activated transcription of WT-Luc while SBZ suppressed it in Jurkat cells. It is consistent with functions of HTLV-1 Tax and HBZ.

Clonal proliferation of STLV-1-infected cells in Japanese macaques

Clonal proliferation of HTLV-1-infected cells has been demonstrated by inverse PCR and next generation sequencing methods [25-27]. We analyzed the clonality of STLV-1-infected cells in seropositive Japanese macaques by identifying the genomic sequences adjacent to the 3' LTR. Briefly, genomic DNAs of monkey PBMCs were sheared by sonication and the integration sites of the provirus adjacent to the viral 3' LTR were amplified by linker-mediated PCR. Thereafter, we massively sequenced the integration sites and analyzed the abundance of each clones according to the method reported by Gillet et al. [27]. The detailed information on the deep sequencing is described in Additional file 2. The clonality of STLV-1-infected cells in three monkeys is shown in Figure 6A. Proviral load is represented as the percentage of STLV-1-infected cells in PBMCs. In monkeys with lower proviral load, a few major clones, together with many minor ones, were observed in Mf-1. Some clones proliferated in Mf-2 (Figure 6A, left

and middle). On the other hand, another monkey, Mf-3, which had higher proviral load (17%), possessed two major STLV-1-infected clones (Figure 6A, right). To study which cell types are infected by STLV-1, Tax expression in PBMCs obtained from one monkey (Mf-4) was analyzed by flow cytometry. The Tax-expressing cells were largely found to be $CD4^+$ T cells, as is the case with HTLV-1 infection in humans (Figure 6B).

STLV-1-associated T-cell lymphoma in a Japanese macaque

A monkey (Mf-4) developed anorexia and had paralysis of the lower limbs. This monkey had high proviral load (53%) in PBMCs. We suspected that this monkey has developed a disease similar to HAM/TSP because paralysis of the lower limbs is one of the major symptoms of HAM/TSP patients. Magnetic resonance imaging (MRI) revealed a high intensity lesion in the brain on a T2-weighted image (Figure 6C). Pathological analysis showed that this tumor was a lymphoma with atypical morphology, and by immunohistochemical methods, it was found that these cells were $CD3^+$ $CD4^+$ (Figure 6D). In contrast, no obvious demyelination was observed in the spinal cord. Thus, this monkey was diagnosed with T-cell lymphoma in the brain rather than the disease like HAM/TSP. In this monkey, some major clones had proliferated in peripheral blood (Figure 6E, left). We found that the major clones in peripheral blood were also detected in the brain lesion (Figure 6E, right). These observations demonstrate that STLV-1 causes lymphoma in Japanese macaques. Notably, one of the major clones in the brain, which had its provirus integration site in chromosome 13, was not detected in PBMCs. This was confirmed by conventional PCR using the primers for the 3'LTR and the host genome proximal to the integration site (Figure 6F). Moreover, a clone with the integration site in chromosome 18 was also detected only in the brain lesion. These tumor-specific

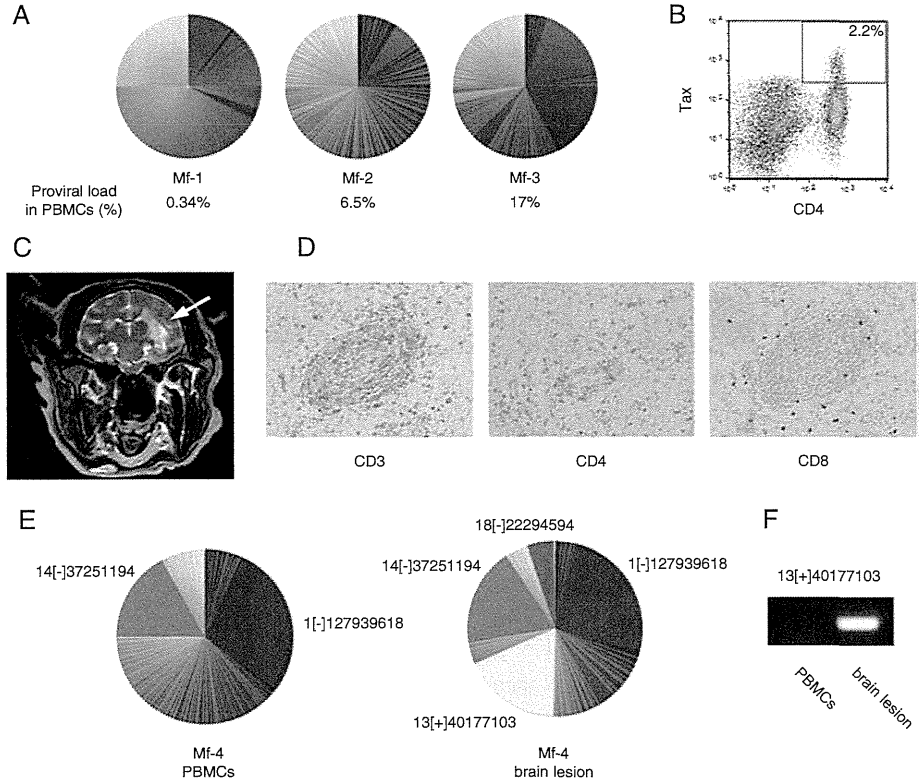

Figure 6 Clonal proliferation of STLV-1-infected cells and lymphomatous lesion in the STLV-1-infected Japanese macaque. (A) The relative frequency of STLV-1^+ clones in three monkeys (Mf-1, Mf-2 and Mf-3) is presented. Each area in the pie charts represents the proportion of provirus in a separate clone (identified by its unique integration site). **(B)** Flow cytometric analysis of PBMCs from an STLV-1-infected monkey shows that Tax-expressing cells are positive for CD4. **(C)** Magnetic resonance imaging of the brain of monkey Mf-4. The lesion is indicated by the white arrow. **(D)** Immunohistochemical analyses show that lymphoma cells are positive for CD3 and CD4. **(E)** Relative abundance of STLV-1^+ clones identified by unique integration sites of the provirus in PBMCs (left) and in the brain lesion (right) of Mf-4. Some of the abundant clones that are observed both in PBMCs and the brain lesion are painted in the same color in the two pie charts. **(F)** STLV-1^+ abundant clone 13[+] 40177103 is detected in the brain lesion by using the primers for 3' LTR and the genomic region, but not in PBMCs.

STLV-1-infected clones are thought to contribute to the formation of the tumor.

Treatment with anti-CCR4 antibody decreased proviral load in STLV-1-infected Japanese macaques

ATL cells express high levels of CC chemokine receptor 4 (CCR4) [28]. Recently, mogamulizumab, a humanized IgG1 monoclonal antibody against CCR4 [29], was approved in Japan for the treatment of relapsed ATL patients. HTLV-1-infected cells of healthy carriers also express CCR4, which indicates that mogamulizumab likely reduces the proviral load in HTLV-1-infected asymptomatic individuals [30]. High proviral load has been reported to be associated with HAM/TSP, HTLV-1 uveitis, and risk of ATL, indicating that mogamulizumab may potentially be used for the treatment of HTLV-1-associated diseases and the prevention of ATL. However, it is not clear whether mogamulizumab can reduce the proviral load in HTLV-1-infected individuals. We confirmed that mogamulizumab also recognizes macaque CCR4 by staining Japanese macaque PBMCs *in vitro* with the fluorescently labeled antibody (see Additional file 3). Then, we tested the efficacy of mogamulizumab to reduce the proviral load in STLV-1-infected Japanese macaques. Mogamulizumab was administered to two monkeys with high proviral load (Mf-6 and Mf-7), once a week for 4 weeks. As shown in Figure 7A, nearly half of the $CD4^+$ T cells expressed CCR4 before the treatment (week 0). After the treatment, the CCR4 positivity decreased to 1.62% and 12.4% respectively. We also

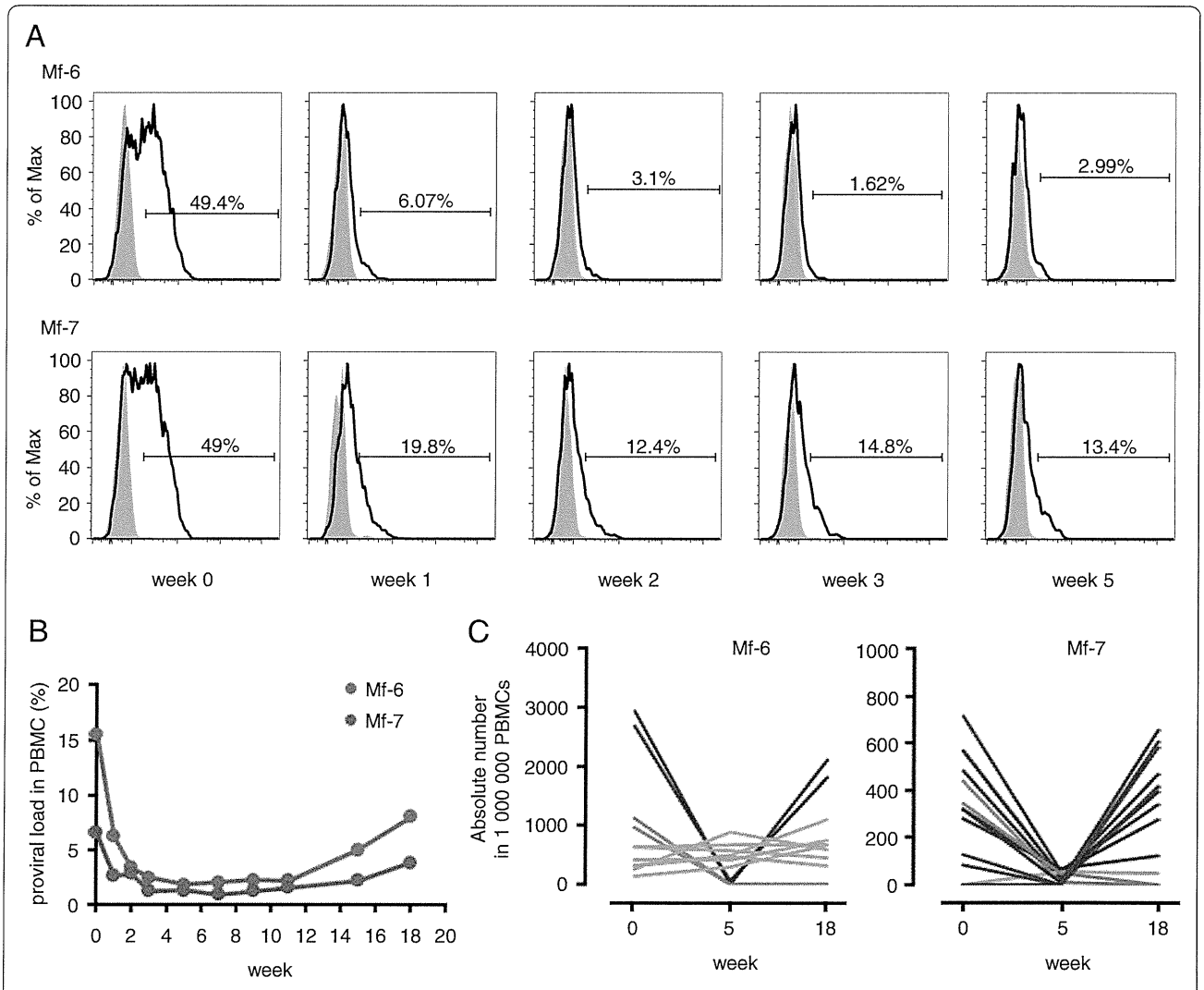

Figure 7 Effect of anti-CCR4 antibody on STLV-1 dynamics *in vivo*. **(A)** $CD3^+CD4^+$ T cells were gated and the expression of CCR4 was analyzed by flow cytometry. **(B)** Changes in STLV-1 proviral load in two monkeys treated with anti-CCR4 antibody until week 3. **(C)** Absolute cell numbers of the five most abundant clones in 1,000,000 PBMCs at weeks 0, 5 and 18 are shown.